

~~RESTRICTED DATA~~
ATOMIC ENERGY ACT OF 1954

NASA TECHNICAL
MEMORANDUM



UB
NASA TM X-1520

UB
NASA TM X-1520

REACTOR PHYSICS CONSIDERATIONS
AND WEIGHT CHARACTERISTICS
OF SMALL WATER-GRAPHITE
NUCLEAR ROCKET REACTORS

NOV 09 2004

CLASSIFICATION CHANGED

To Unclassified

By authority of H. H. Mairies

Date Jan. 3, 1973
per lmd

by M. Ray Clark
Lewis Research Center
Cleveland, Ohio

LIBRARY COPY

FEB 4 1968

LEWIS LIBRARY, NASA
CLEVELAND, OHIO

NATIONAL AERONAUTICS AND SPACE ADMINISTRATION • WASHINGTON, D. C. • MARCH 1968

REACTOR PHYSICS CONSIDERATIONS AND WEIGHT CHARACTERISTICS
OF SMALL WATER-GRAPHITE NUCLEAR ROCKET REACTORS

By M. Ray Clark

Lewis Research Center
Cleveland, Ohio

RESTRICTED DATA

ATOMIC ENERGY ACT OF 1954

GROUP 1
Excluded from automatic
downgrading and declassification

CLASSIFIED DOCUMENT-TITLE UNCLASSIFIED

This material contains information affecting the national defense of the United States within the meaning of the espionage laws, Title 18, U.S.C., Secs. 793 and 794, the transmission or revelation of which in any manner to an unauthorized person is prohibited by law.

NOTICE

This document should not be returned after it has satisfied your requirements. It may be disposed of in accordance with your local security regulations or the appropriate provisions of the Industrial Security Manual for Safe-Guarding Classified Information.

NATIONAL AERONAUTICS AND SPACE ADMINISTRATION



CONTENTS

	Page
SUMMARY	1
INTRODUCTION	2
DESCRIPTION OF BASIC CORE GEOMETRY	3
Basic NERVA Fuel Element	3
Geometrical Variations and Water Volume Fraction	5
FUEL-ELEMENT DESIGN LIMITATIONS	7
Maximum Power Density	7
Fuel-Loading Limit and Fissionable Isotopes	8
ESTIMATION OF REACTIVITY AND CONTROL REQUIREMENTS	10
SMALL WATER-GRAPHITE CORE REACTIVITY	12
Axial Reactor Geometry and Reactivity Approximation	12
Water Volume Fraction Effect on Basic Reactivity and Performance	13
Initial conditions	13
Reactor power variation	15
Reactor power-weight variation	15
Potential weight-reduction variables	16
Selection of water volume fraction and core geometry	16
Core-void-fraction variation	17
Zero-water-volume-fraction case	17
Detailed Calculation of Selected Core Geometry	18
Reactivity-limited core sizes	22
Core sizes greater than 400 megawatts	22
Control-reactivity limitations	22
POWER DISTRIBUTION OF SMALL CORES	23
Gross Radial Power Distribution	24
Cell Power Distribution	26
Axial Power Distribution	27
TEMPERATURE DEFECT OF SELECTED CORE SIZES	29
SMALL WATER-GRAPHITE REACTOR WEIGHT ESTIMATE	30
AREAS FOR FURTHER STUDY	32

[REDACTED]

SUMMARY OF RESULTS 33

APPENDIXES

 A - DESCRIPTION OF REACTOR CALCULATIONS 35

 B - SPECTRAL-NEUTRON FLUX AND POWER-DISTRIBUTION
 CHARACTERISTICS 42

 C - AXIAL HEAT-TRANSFER COMPARISON 45

REFERENCES 48

[REDACTED]

~~CONFIDENTIAL~~

REACTOR PHYSICS CONSIDERATIONS AND WEIGHT CHARACTERISTICS OF SMALL WATER-GRAPHITE NUCLEAR ROCKET REACTORS (U)

by M. Ray Clark
Lewis Research Center

SUMMARY

A study of small low-thrust nuclear rockets of 200 to 600 megawatts was prompted by the potential application as upper-stage propulsion for unmanned space missions. The choice of small water-graphite reactors stemmed from (1) past studies at Lewis of a range of tungsten water-moderated nuclear reactor sizes and (2) potential development-time reduction by employing the extensive Phoebus-NERVA graphite-fuel-element experience.

The initial analysis selected an optimum power-weight-ratio design in the 200-megawatt power range. The water content and a uranium 233 (U^{233}) fuel loading of 0.7 gram per cubic centimeter maximized the reactivity potential. Maximum power density of Phoebus II-NERVA II technology and a 99-centimeter axially power-tailored core were assumed. The selected fuel-element design was consistent with the NERVA II hexagonal fuel element with minor modifications for the enlarged central tie-tube and water region.

Limitations were then applied to the selected 0.1294-volume-fraction core design for various core sizes in the 250- to 430 megawatt power range. These limitations were a 16.5 percent $\Delta k/k$ reactivity requirement, an 8 percent $\Delta k/k$ control requirement, and a power-gradient restriction. Reactors of less than 250 megawatts power are rejected because of an excessive radial core-reflector interface power gradient. From about 250 to 430 megawatts the reactors are excess-reactivity limited and require appropriate radial reflector thicknesses. Beyond about 400 megawatts the reactors are drum-control-reactivity limited, and the excess reactivity exceeds the requirement and thus allows further design changes. Based on these calculations, a reactor weight of 575 to 750 kilograms in the 250- to 430-megawatt power range was estimated; this weight was extrapolated to 1650 kilograms at 1000 megawatts by reference to NERVA I reactor weight uprated to NERVA II power density.

~~CONFIDENTIAL~~

INTRODUCTION

An extensive research and development effort in nuclear rocket technology is currently centered about the use of graphite for a high-temperature (approx. 2780°K or 5000°R), short-lifetime (approx. 30 min) reactor fuel element. The nuclear rocket reactors employing this type of fuel element are of relatively high power compared with the small nuclear rocket reactors with which this report deals. The NERVA II nuclear rocket reactor (ref. 1) is the most recent design, with reactor power of approximately 5000 megawatts and thrust of 1.11×10^6 newtons (250 000 lb). NERVA II is being developed with two typical propulsion applications in mind, a manned Mars mission and lunar support operations (ref. 2). Extensive graphite-fuel-element development in connection with the program has demonstrated fuel-element operation in reactors for a duration of about 30 minutes at temperatures approaching the desired maximum fuel-element temperature (e.g., ref. 3, p. 8).

Concurrently, the feasibility of two other nuclear rocket concepts employing tungsten fuel elements has been studied to a smaller degree, with no actual fuel-element operation in reactors. A water-moderated, thermal-neutron spectrum reactor of 1500 megawatts power (ref. 3) and a fast-neutron spectrum reactor of 2000 megawatts power (ref. 4) have been studied at NASA Lewis and the Argonne National Laboratory, respectively. Some study was devoted in both these conceptual areas to smaller reactors in the 200-megawatt range, as an outgrowth of the higher-power designs (refs. 3 and 4). At Lewis this effort evolved into a study of the small water-graphite nuclear rockets with which this report is concerned, in order to take advantage of the extensive graphite-fuel-element development in the 200-megawatt power range, as well as at the higher powers.

The interest in smaller, lower-thrust nuclear rockets (power, 200 to 600 MW; thrust, 44 500 to 133 000 N (10 000 to 30 000 lb)) stems from their potential application as upper-stage propulsion for possible unmanned missions in the 113- to 13 600-kilogram (250- to 30 000-lb) payload range. This report defines the reactor physics and reactor weight characteristics of such a class of small reactors in a preliminary fashion to contribute to the evaluation of these nuclear rockets for unmanned missions.

The general characteristics of nuclear rockets as compared with chemical rockets are (1) their heavier engine weight for the same thrust and (2) the existence of a minimum reactor size and, therefore, a minimum weight and associated thrust because of the nuclear criticality limitation. However, in terms of rocket performance, minimum size and low thrust require long operating time, and longer operating time for the same total impulse can require a propellant weight increase because of "gravity loss". (The fuel-material lifetime at high temperature provides an upper limit on this reactor operation time as well.) Thus, the nuclear rocket performance evaluation must consider a

CONFIDENTIAL

range of reactor weight and thrust for optimization of performance between the two competing effects, nuclear engine weight and propellant-weight gravity loss. This report, therefore, deals with a range of small reactor sizes rather than with just the minimum size.

In this study the minimum size of the basic NERVA type of graphite reactor was reduced by defining a class of reactors where water is incorporated in the reactor core. The water content improves the neutron thermalization properties of graphite and results in a large increase in reactivity, which may be used for core size reduction.

The basic aspects of the NERVA fuel-element technology needed for this analysis are first presented along with the method of incorporating the water-flow loop. The excess reactivity and control requirements for the small water-graphite reactors are then developed as criteria for the reactivity aspects of the analysis. The analysis itself consists of two phases:

(1) Reactivity variations were calculated for varying core geometry and water volume fraction and used to define the optimum water volume fraction that gives the best reactor power-to-weight ratio in the 200 megawatt power range. The excess-reactivity criterion was applied in this analysis to obtain the thickness variation of the radial reflector, the primary weight variable for these reactivity-limited reactors.

(2) With the previously selected core geometry and water volume fraction held constant, the other reactor characteristics were studied in more detail. The core size was varied over a power range of 200 to 400 megawatts. Drum-control-reactivity and power-gradient criteria, as well as the basic reactivity requirement, were applied in the reactor analysis to determine the limitations of the core design with variable size.

The temperature-defect reactivity change from ambient to operating temperature was estimated from calculations for the selected core geometry and water volume fraction because of the strong dependence of this value on the degree of water moderation. This value was used in the general excess- and control-reactivity criteria to provide a reasonable estimate for this reactor type. Reactor weight as a function of reactor power was then estimated from the data on the selected core geometry to contribute to the evaluation of these nuclear rockets in unmanned missions.

DESCRIPTION OF BASIC CORE GEOMETRY

Basic NERVA Fuel Element

The basic NERVA fuel element is shown in figure 1. It is a hexagonal extruded fuel element with 19 coolant holes coated with about 0.025 to 0.05 millimeter (1 to 2 mils) of niobium carbide (NbC). The holes are equally spaced in a triangular array. The hole

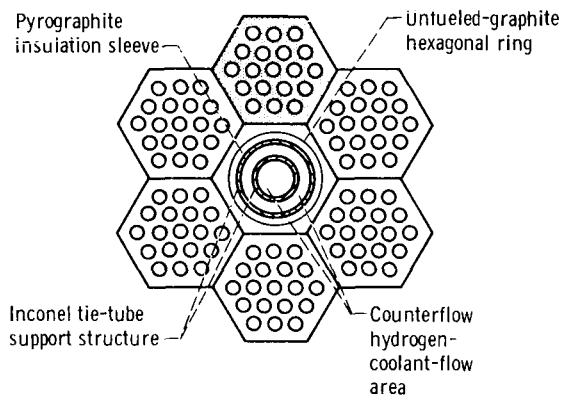
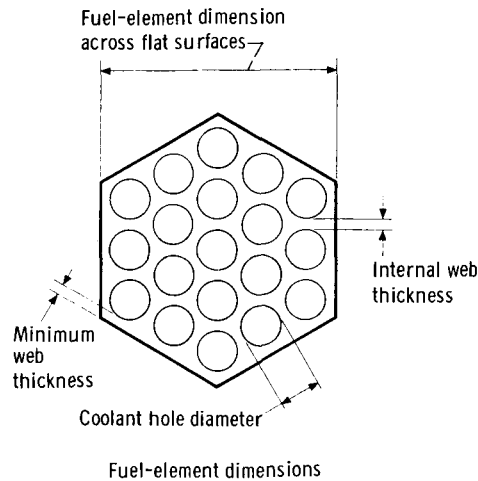


Figure 1. - Basic Phoebus- NERVA fuel element. Basic building block of reactor core, cluster of six fuel elements around unfueled central hexagon.

size and minimum web thickness between holes were optimized for the maximum allowable power density consistent with the estimated thermal stress limitations of the fueled graphite and with the hydrogen pressure drop of the reactor core. The same graphite-fuel-element geometry was used as much as possible for the small water-graphite nuclear rocket in order to take advantage of the extensive fuel-element development for the Phoebus-NERVA program.

The basic building block of the core, shown in figure 1, is the cluster of six fuel elements around a central unfueled hexagon. A counterflow tie-tube passes axially through a thermally insulating pyrographite sleeve within the unfueled central hexagon and is suspended from a support plate at the inlet end of the reactor (fig. 2). This tie tube supports the pressure drop and friction loads of the fuel elements by a support block attached to the hot end of the tie tube and extends beneath the hot ends of the clustered fuel elements.

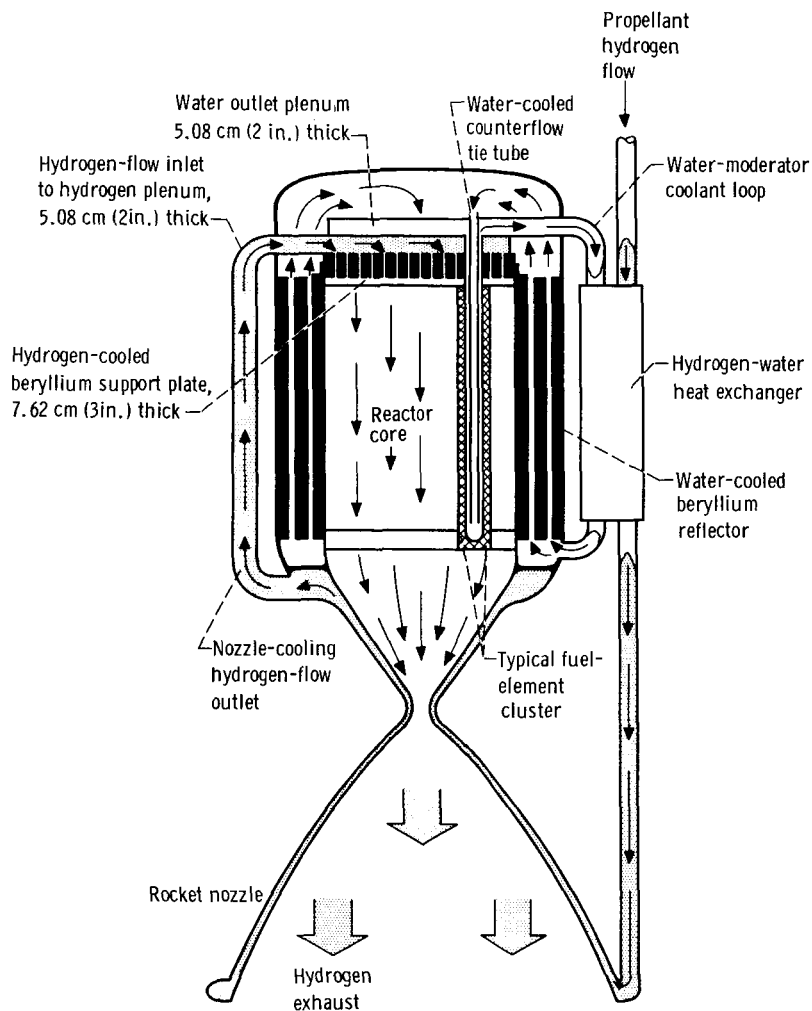
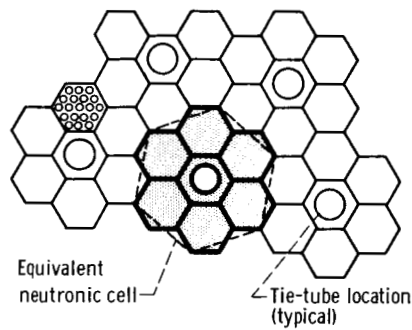


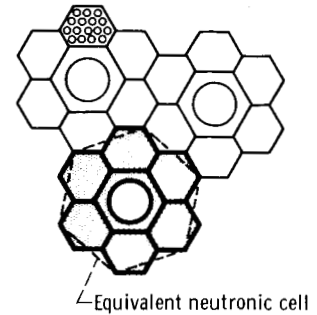
Figure 2. - General arrangement of small water-graphite nuclear rocket.

Geometrical Variations and Water Volume Fraction

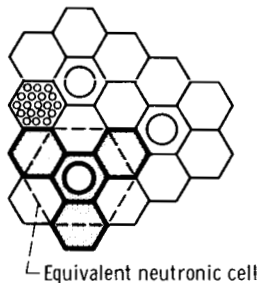
The most convenient location for introduction of water, to maintain the basic design of the NERVA core, is the tie-tube area. The adequate heat capacity and heat transfer of water allow the substitution of a water-flow loop through the tie tubes and accompanying heat exchanger (fig. 2) for the hydrogen flow of the current single-fluid coolant system. However, the present tie-tube diameter provides a low volume fraction of water in the core. Increasing the water volume fraction, therefore, requires enlarging the tie-tube diameters and the central unfueled hexagon. This increase in water volume fraction is at the expense of fuel-element area if the optimized hole size and web thickness are



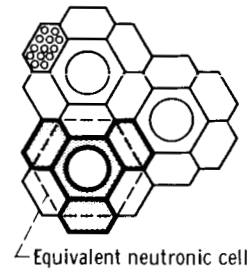
(a) Phobus-NERVA design,
0.0488 water volume fraction.



(b) Four coolant-hole rows in fuel element,
0.1294 water volume fraction.



(c) Three-fuel-element cluster,
0.0854 water volume fraction.



(d) Three-fuel-element cluster,
0.230 water volume fraction.

Figure 3. - Water volume fraction of geometrical variations in reactor core.
(Crosshatching denotes basic fuel-element cluster.)

to be maintained. Figure 3 shows some variations of the basic geometry which allow increases of the water volume fraction.

The NERVA fuel-element cluster and tie-tube diameter presented in figure 3(a) would provide an 0.0488 water volume fraction in the core. The six-element cluster was maintained and the central tie-tube region was expanded by removing successive rows of coolant holes in the adjacent fuel elements. Figure 3(b) illustrates the increase to 0.1294 water volume fraction when one row of three coolant holes was removed. Removal of two rows of coolant holes (not shown) would produce a 0.2482 water volume fraction, which is not sufficiently different from the 0.230 case (described next) to be considered in these preliminary calculations.

By altering support block geometry and reverting to a three-fuel-element cluster, intermediate water volume fractions are possible, as shown by figure 3(c) and (d) for water volume fractions of 0.0854 and 0.230, respectively. While the tie tubes are still in a triangular array among the fuel elements, their pitch is correspondingly less than in figure 3(a) and (b). The clusters are now triangular in shape as shown, and fuel elements are shared between the effective nuclear cell areas of this geometry (also shown in fig. 3).

[REDACTED]

This range of water volume fraction, 0.0488 to 0.23, is of concern herein. The fuel-element fabrication technique is basically unaltered in any of the geometries, but die sizes would have to be altered or enlarged to produce (1) irregular hexagonal fuel elements, whose area is a portion of the regular hexagonal fuel element and (2) the enlarged unfueled hexagon surrounding the central tie tube. Depending on the final choice of geometry, some redesign of the support block may also be necessary as in the geometries shown in figure 3(c) and (d).

The introduction of the water-flow loop may necessitate the review and perhaps modification of the tie-tube design to ensure a greater degree of leak-tightness for the water-flow system in the area of the high-temperature core. Whereas hydrogen corrosion would have been the result of hydrogen leakage in the tie-tube area, a water leak impinging on the hot fuel elements might produce a catastrophic type of failure by the sudden explosive production of steam. This problem requires further study.

FUEL-ELEMENT DESIGN LIMITATIONS

Several limitations were imposed on the fuel-element design of the small nuclear rocket to ensure compatibility with Phoebus-NERVA fuel-element state of the art and anticipated development.

Maximum Power Density

The first limitation is the estimated maximum allowable power density of the fuel element. The dimensions of the Phoebus-NERVA fuel element were selected after careful consideration of several design aspects. These aspects are the minimum fabricable web thickness, the core hydrogen pressure drop, and the thermal stress limit of the fueled graphite. A typical design analysis is reported in reference 5 for early studies of the Phoebus reactor. Through such a combined analysis, the optimum internal web thickness b and coolant-hole diameter d of the fuel element were selected to satisfy all three design aspects and to obtain the maximum allowable power density for these conditions. (Power density $(Pd)_{fm}$ refers to the fission-produced power density within the solid fueled-graphite material around the coolant holes of the fuel element.) Since these same design aspects were applied to the small nuclear rocket, the current optimized dimensions for the NERVA II reactor were used directly in this study. Thus, the current maximum allowable power density was applied to the small nuclear rocket.

In reference 1 (p. 2-16), the average core power density of the NERVA II and

[REDACTED]

CONFIDENTIAL

Phoebus II designs are given as 61 and 70 megawatts per cubic foot (2160 and 2470 MW/m³), respectively. Considering these fuel-element geometries and assuming radial and axial maximum-to-average power factors of 1.2 and 1.362 (ref. 5) result in maximum allowable fueled-material power densities of 6.84 and 7.48 kilowatts per cubic centimeter (106 and 116 Btu/(sec)(in.³)) for the NERVA II and Phoebus II designs, respectively. The NERVA II value was used to estimate the small reactor powers.

The corresponding fuel-element dimensions which were used in this study are those for the NERVA II, given in reference 1 (p. 2-16) as follows:

Dimension across flat surface of hexagonal fuel element, F, cm (in.) . . .	1.915 (0.754)
Internal web thickness, b, cm (in.)	0.133 (0.0524)
Coolant-hole diameter, d, cm (in.)	0.292 (0.115)
Minimum web thickness at fuel-element edge, w, cm (in.)	0.0762 (0.030)

The minimum web thickness for the fabrication limitation occurred along the fuel-element edge and was held constant independent of internal web thickness and coolant-hole diameter variations.

Because of the low level of allowable thermal stress, the primary design limitation for these fuel-element dimensions is caused more by the thermal stress limit than the pressure drop limit. In reference 5, the thermal stress is expressed in terms of the parameter ΔT_s (the temperature difference from the coolant-channel surface to the corner of the hexagonal area surrounding the coolant hole) and is determined by heat-transfer calculations for a single coolant-hole cell in the fuel element. The ΔT_s data from figures 2(a) to 5(a) of reference 5 were plotted as the internal web thickness b against coolant-hole diameter d for constant ΔT_s and $(Pd)_{fm}$ (figs. 4(a) to (c)). The allowable fueled-material power densities established for NERVA II and Phoebus II were compared. Values of ΔT_s of about 91.6° and 117° K (165° and 210° R) were deduced for the current NERVA II and Phoebus II designs, respectively (fig. 4(d)). The variation of $(Pd)_{fm}$ as a function of ΔT_s derived from the crossplotting is presented in figure 4(d) to allow for future uprating of the small nuclear rockets in the event the thermal-stress or ΔT_s limit is raised. A simple ratio of allowable power densities gives the power scaling factor for uprating if pressure drop is assumed to be satisfactory.

Fuel-Loading Limit and Fissionable Isotopes

Current maximum fuel loading in the graphite is about 0.4 gram of uranium per cubic centimeter (ref. 1, p. 2-16). In this study, the maximum fuel loading considered possible for current technology is 0.7 gram per cubic centimeter. (Private communication of S. J. Kaufman of Lewis with F. C. Schwenk of AEC-NASA Space Nuclear Propulsion Office indicated a maximum potential loading of about 0.75 to 0.80 g/cu cm.) A

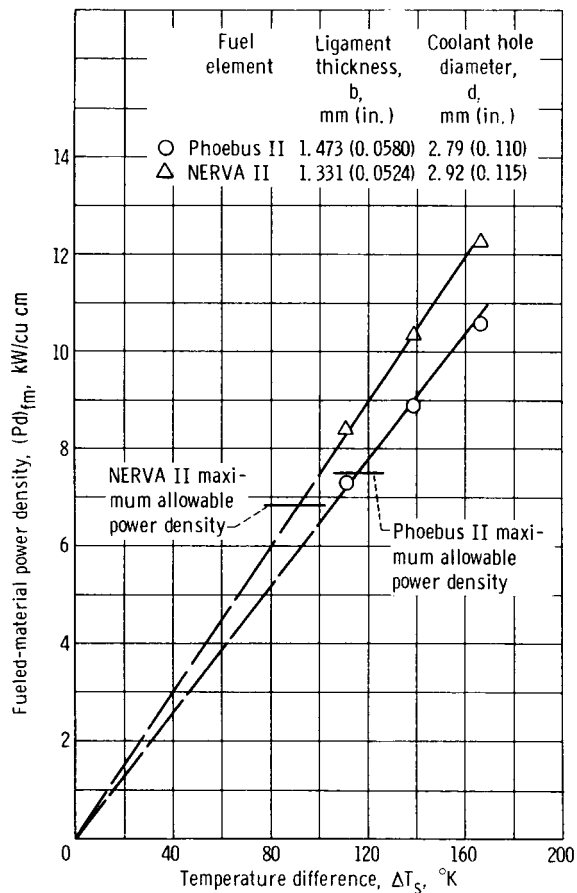
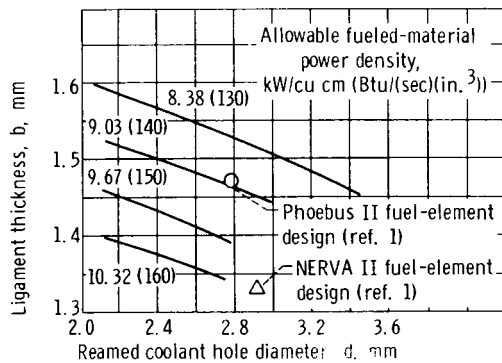
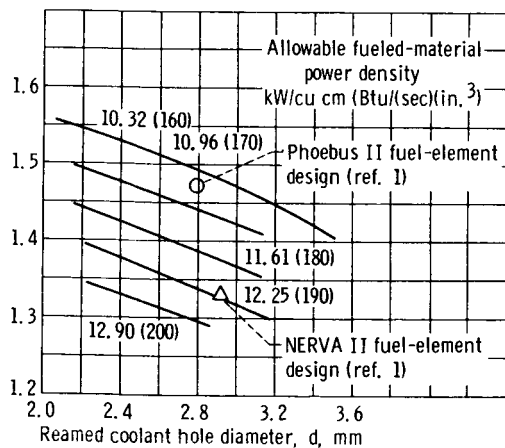
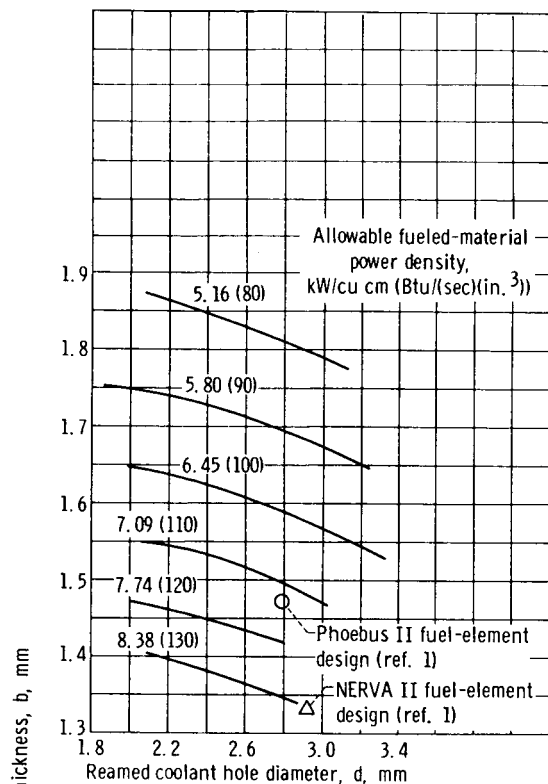


Figure 4. - Fuel-element geometry as function of power density and thermal stress limits.

recent report (ref. 6, p. 34) indicates that tests are being performed to determine the practicality for reactor design of loadings of 0.75 and 1.0 gram per cubic centimeter.

Any isotope of uranium can be used in the fuel element, from the chemical standpoint. Not only U^{235} but also U^{233} were therefore considered. The gamma activity associated with U^{233} fuel requires some change in handling techniques in fuel-element fabrication, but this modification may be reasonable (e.g., ref. 7). Uranium 233 activity is dependent on U^{232} content, and production of U^{233} with only a few parts per million U^{232} is available. Therefore, radiation levels would be substantially lower than the already reasonable levels given in reference 7 for 42-ppm U^{232} .

ESTIMATION OF REACTIVITY AND CONTROL REQUIREMENTS

When considering size and core-composition limitations due to reactor criticality, sufficient excess reactivity allowance must be made to provide for operational and detailed design aspects beyond the scope of the preliminary reactivity calculations. These reactivity requirements are for temperature-defect reactivity, operation fuel loss, xenon 135 poisoning, fabrication tolerances, axial power shaping, and local or gross radial power flattening. The control requirement can also be estimated by using those reactivity requirements applicable to the reactor control and adding a reactivity requirement for shutdown margin.

The preliminary percentage $\Delta k/k$ estimates of the reactivity requirements are as follows:

Axial power tailoring	4
Local and gross radial power flattening	5
Excess reactivity for fuel loss, xenon poisoning,	
fabrication tolerances, etc.	2.5
Total temperature defect	3.5

for a total reactivity requirement of 15.0 percent $\Delta k/k$. A 1.5 percent $\Delta k/k$ conservative margin for calculation accuracy, etc., was added to bring the complete reactivity requirement to 16.5 percent $\Delta k/k$.

Axial power tailoring, the first reactivity requirement, allowed reduction of the Phoebus-NERVA 52-inch (132-cm) fuel-element length by improving axial heat transfer to approximate more closely axially constant wall-temperature heat transfer to the coolant. This condition minimized the required heat-transfer length for given exit and inlet temperatures by maximizing local heat transfer. Also it afforded a more compact core

[REDACTED]

geometry (closer to $L/D = 1$) to take maximum advantage of axial reflectors and the structure above the core diameter for shielding purposes.


The axial power shaping (or tailoring) could be accomplished by axially zoned fuel-loading variations or neutronic poison variations. Tantalum, currently employed as a nuclear shimming poison in the unfueled central hexagon of the basic fuel-element cluster for Phoebus designs, illustrates the poison technique. However, a thermal absorber like boron may need to be considered in this application. The reactivity estimate was based on analytical experience with axial power tailoring of the tungsten water-moderated nuclear rocket. In that case, the power distribution peak was already shifted toward the reactor core inlet by use of an axial inlet reflector, and 4 percent reactivity for fuel zoning was required to complete the necessary tailoring (e.g., ref. 3, p. 193 ff).

The reactivity estimate for the next requirement was similarly obtained from tungsten water-moderated nuclear rocket analysis experience. The gross radial power flattening is performed to minimize the ratio of maximum-to-average core power density and to allow more of the radial core area to operate at the maximum power-density limit. Local power flattening may be necessary for the same reason if detailed local power distribution, as for example the neutronic cell equivalent of central tie-tube water region and clustered fuel elements, shows nonuniformity initially. However, calculations reported in the section POWER DISTRIBUTION OF SMALL CORES show that cell power flattening is unnecessary.

The 2.5 percent excess reactivity allowed for a variety of reactivity loss conditions does not include enough reactivity for peak xenon override, which could be as much as 8 percent in worth depending on the degree of thermalization of the neutron spectrum with water content. Therefore, the reactor may be excluded from operation for a period of time after shutdown, although only single-start operations are anticipated for this reactor. Immediate restarts in case of accidental shutdown are not ruled out provided the restart occurs within minutes.

The 3.5 percent excess reactivity for temperature defect accounts for reactivity changes (generally negative) caused by increased radial leakage, thermal expansion, and shifting thermal-neutron spectrum as the reactor increases in temperature to operating conditions. The tungsten reactor analysis required about 2.8 percent reactivity for temperature defect, but calculations reported in the section TEMPERATURE DEFECT OF SELECTED CORE SIZES indicated that about 3.5 percent excess reactivity is required for this reactor design. A 1.5 percent excess reactivity was added to the reactivity requirements to ensure conservatism in reactor size limitations and to allow for inaccuracy in reactor calculational models, cross sections, methods, etc.

The estimated control requirements in percentage $\Delta k/k$ of reactivity are as follows:



Excess reactivity for fuel loss, xenon poisoning, fabrication tolerances, etc.	2.5
Total temperature defect	3.5
Shutdown margin	2.0

for a total drum control requirement of 8 percent $\Delta k/k$. Reflector drum control must increase reactivity through this range in proceeding from the cold shutdown condition to the hot critical operational conditions.

The inclusion of hydrogen density effects in the reactivity and control requirements was neglected. The introduction of full-power hydrogen density into the coolant channels increases reactivity. However, the effect is fairly small (about 2 percent $\Delta k/k$ for NERVA II design, ref. 1, pp. 5-8; less for more thermalized neutron spectra) for normal operating conditions and would therefore reduce reactivity and control requirements little, if any.

SMALL WATER-GRAPHITE CORE REACTIVITY

Preliminary calculations were first performed to establish which of the four possible core designs over the range of 0.0488 to 0.230 water volume fraction should be studied in further detail. The optimum reactor design at any given reactor power must have a maximum power-weight ratio and the required excess reactivity. In applying these criteria to selection of one of the four core designs, core diameter rather than reactor power was maintained constant, and the optimization was performed at a core diameter typical of the low power end of the power range for small nuclear rockets. This procedure was used to minimize the number of these preliminary calculations, but the optimization was the same as for constant reactor power and is expected to apply at moderately higher powers as well.

Axial Reactor Geometry and Reactivity Approximation

In all the calculations that follow, the axial geometry is represented in a simplified way in order to use exclusively radial one-dimensional calculations for this study. An unreflected axial length of 132 centimeters (52 in.) similar to the Phoebus-NERVA fuel-element length was used and was assumed to be equivalent in reactivity effect to the actual geometry. The actual axial geometry is a shortened core length of about 99 centimeters (39 in.) (for the axially power-tailored condition) with axial reflection at the core inlet end from a beryllium support plate and from the tie-tube water inlet and outlet plenums. Figure 2 (p. 5) shows the general arrangement of the axial reflector regions,

[REDACTED]

core fuel-element clusters, and tie tubes in relation to the complete reactor and flow systems.

As a check of the reactivity aspects of these axial geometry assumptions, a set of axial calculations representing the 132-centimeter (52-in.) bare core and 99-centimeter (39-in.) axially reflected core before final power tailoring were later performed for the 0.1294-water-volume-fraction core geometry. The 132-centimeter (52-in.) bare-core reactivity was about 2.2 percent greater than for the 99-centimeter (39-in.) axially reflected core, when including the reflector poisoning due to tie tubes, plenums, and orifice structure. The 2.2 percent difference is expected to be a constant bias in all the preliminary calculations and should not effect the choice of optimum water volume fraction.

Water Volume Fraction Effect on Basic Reactivity and Performance

Preliminary calculations were made to estimate the reactivity variation over the range of water volume fraction from 0.0488 to 0.230 and corresponding core geometries. From the estimated excess reactivity requirement, 16.5 percent $\Delta k/k$, or 0.18 Δk , is required of an acceptable reactor design. (All the reactivity values in this report are defined as $\Delta k/k$ where k is the average of k_{eff} (effective multiplication factor) values defining the change Δk . This definition of reactivity requirements and application to cold, clean reactors with calculated k_{eff} values of the order of 1.2 assumes that to first order the values are preserved and are applicable to reactors in the operating condition.)

Initial conditions. - Initially, the U^{233} fuel loading was set at an upper limit of 0.7 gram per cubic centimeter, and a maximum radial reflector thickness of 12.7 centimeters (5 in.) was chosen. This thickness approaches an infinite reflector. Further thickness increases result in essentially deadweight additions for constant core diameter since the reactivity increase is marginal and the reactor power-weight ratio decreases. The radial reflector composition of 90 volume percent beryllium and 10 volume percent water was selected from tungsten water-moderated reactor design experience to represent a water-cooled reflector. This choice of fuel loading and radial reflector thickness maximized the reactivity obtainable from a given core size and design and, therefore, allowed a comparison of excess reactivity of the four geometrical core variations shown in figure 3. The results of this reactivity comparison are shown in figure 5. A constant core diameter of 36.4 centimeters (14.33 in.) was arbitrarily selected to consider the reactivity variations in the range of 200 megawatts of reactor power, which is considered about the minimum power for useful small nuclear rocket stage performance. Further studies of the selected core design show the core diameter for the 200-megawatt

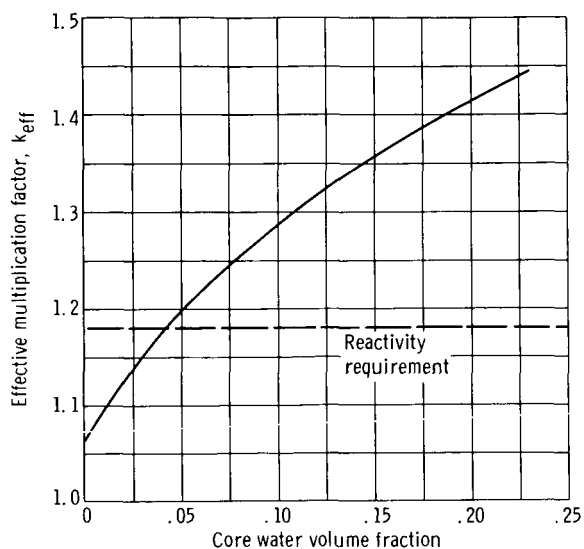


Figure 5. - Basic reactivity of graphite-water-uranium 233 fuel elements. Radial reflector composition, 90 volume percent beryllium and 10 volume percent water; reflector thickness, 12.7 centimeters; core axial length, 132 centimeters; uranium 233 content, 0.7 gram per cubic centimeter; no cell flux weighting.

TABLE I. - REACTOR POWER AND POWER-DENSITY
VARIATION WITH WATER VOLUME FRACTION

[Core length, 99 cm (39 in.); constant core diameter, 36.4 cm (14.33 in.); assumed radial and axial maximum-to-average power factors, 1.2 and 1.362; maximum allowable fueled-material power density, 6.84 kW/cu cm (106 Btu/(sec)(in.³)).]

Water volume fraction, vol. %	Core fueled-material volume fraction	Core average power density, kW/cu cm	Reactor power, MW	Core void fraction
4.88	0.5175	2.163	223	0.3278
8.54	.4531	1.893	194	.2869
12.94	.4384	1.833	189	.2777
23.0	.3152	1.320	136	.1997
0	.5175	2.163	223	.3766

range to be about the minimum because of reactor design limitations as well. The volume fractions and atom densities for the four cases as well as a description of the reactor calculation method, are given in appendix A. In appendix B, the range of the neutron flux spectrum variation with water volume fraction is given.

Reactor power variation. - As the multiplication factor k_{eff} increases with increasing water volume fraction, as shown in figure 5 for a fixed core diameter, the reactor power decreases. As shown in table I, with the maximum allowable fueled-material power density held constant, the core average power density and the reactor power are altered according to the water volume fraction in the core.

Reactor power-weight variation. - The variation of reactor power-weight ratio with water volume fraction can be established if the radial reflector thickness as a major reactor weight component is allowed to decrease to attain just the required reactivity in each case. Then, the variation of reactivity with water content can be weighed against the gain or loss in power-weight ratio.

TABLE II. - REACTOR WEIGHT AND POWER-WEIGHT RATIO
VARIATION WITH WATER VOLUME FRACTION

[NbC coating neglected; constant core diameter, 36.4 cm (14.3 in.);
core length, 99 cm (39 in.); k_{eff} , 1.18.]

Water volume fraction, vol. %	Core density, g/cu cm	Core weight		Radial reflector thickness, cm	Radial reflector weight		Axial reflector weight		Main water plenum weight		Reactor weight		Reactor power-weight ratio	
		kg	lb		kg	lb	kg	lb	kg	lb	kg	lb	MW/kg	MW/lb
4.88	1.539	159	350	12.1	325	717	34.1	75.3	50.8	112	569	1254	0.391	0.177
8.54	1.589	163	361	9.9	258	569	34.1	75.3	40.1	88.5	496	1094	.393	.178
12.94	1.548	160	352	7.5	184	407	34.1	75.3	28.8	63.5	407	898	.466	.211
23.0	1.602	165	364	4.0	91	201	34.1	75.3	14.1	31.2	305	672	.446	.202

When compared with the estimated reactivity requirement in figure 5, the 0.0488-water-volume-fraction design has just enough reactivity (k_{eff} , 1.195) and would allow almost no reflector thickness reduction. This design represents the unaltered current Phoebus-NERVA fuel-element and tie-tube designs. The power-to-reactor weight ratio for this design was developed and is given in table II.

The other three designs of higher water volume fraction all allow some degree of reflector thickness reduction because of their excess reactivity above the requirement. Calculations of reactivity variation with reflector thickness were performed, the thickness which met the reactivity requirement in each case was selected, and the power-to-reactor weight ratio was developed (table II) to complete the optimization in these cases.

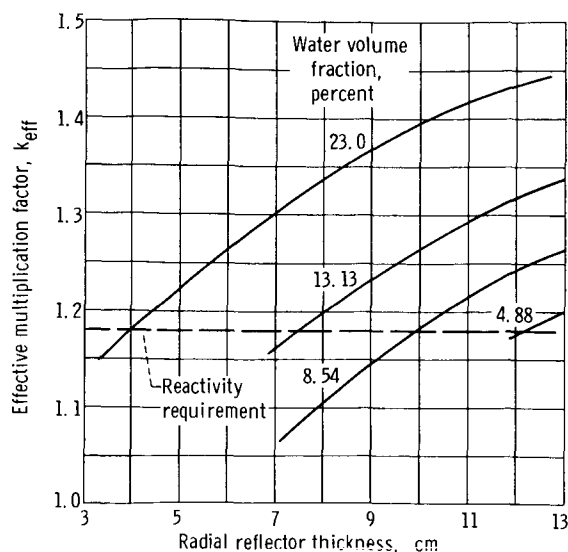


Figure 6. - Reactivity variation with water volume fraction.

TABLE III. - ASYMPTOTIC REACTOR

POWER-WEIGHT RATIO AT

LARGE CORE DIAMETERS

[Power and weight data from
tables I and II.]

Water volume fraction, vol. %	Reactor power-weight ratio	
	MW/kg	MW/lb
4.88	1.16	0.525
8.54	.982	.445
12.94	.975	.442
23.0	.684	.310

The calculated reactivity variations are shown in figure 6. The high leakage of these small cores results in rapid reactivity loss with reflector thickness reduction.

Potential weight-reduction variables. - Only the major weight components were used for the preliminary reactor weight estimation (table II). At reflector thicknesses of about 12 centimeters, the radial reflector weight is the predominant weight component by a factor of 2 compared with core weight, the next largest component. This fact illustrates the importance of the radial reflector thickness as the primary variable for weight reduction of small reactors which exhibit high radial leakage and are reactivity limited.

Another possible weight-reduction variable is fuel loading, but a reduction of fuel loading from 0.7 to 0.4 gram per cubic centimeter represents only about a 9- to 14-kilogram (20- to 30-lb) weight reduction for these cores, a small weight reduction relative to core weight.

Selection of water volume fraction and core geometry. - The core design with 0.1294 water volume fraction exhibited the best power-to-weight ratio and was therefore selected for detailed calculations over a range of reactor powers with about the 200-megawatt level as a minimum. This optimization was assumed to apply for moderate reactor-size and power increases. At large core sizes, however, the reactors are no longer reactivity limited, and the power-weight ratio approaches an asymptotic value determined primarily by the axial reflector and core weights. The radial reflector decreases to some thickness required for the radial power flattening of the circumferential core (assuming other means of control are found or reflector control is still adequate), and the radial reflector is a small part of the total weight at large diameters. Table III indicates that the 4.88-volume-percent-water design would then become optimum.

Core-void-fraction variation. - The basic reactivity variation in figure 6 for the four geometrical variations of core design also includes the effects of core-void-fraction variation, another strong reactivity variable besides water volume fraction. This variation of the core void fraction was expected, however, since the optimum fuel-element geometry (for maximum power density) including coolant-hole diameter was maintained as a constant while the water and fuel-element volume fractions in the cores were varied. The last column in table I (p. 14) shows the void volume fraction for the different cores. Reducing the void fraction in the 0.0488-water-volume-fraction core, for example, by reducing coolant-hole diameter and basic fuel-element size could increase the reactivity, but this procedure would violate the assumption of the constant optimum fuel-element geometry from Phoebus II-NERVA II technology.

Zero-water-volume-fraction case. - Excess reactivity was calculated for the basic Phoebus-NERVA core geometry without the water in the tie tubes, using the same cross sections and methods, to illustrate the need for the water moderator in these small cores (see table I and fig. 5, p. 14). Even with U^{233} fuel and the assumed maximum fuel loading and maximum radial reflector thickness, the excess reactivity above cold critical was only about 5.8 percent $\Delta k/k$ for the 200-megawatt reactor. Reduction of the

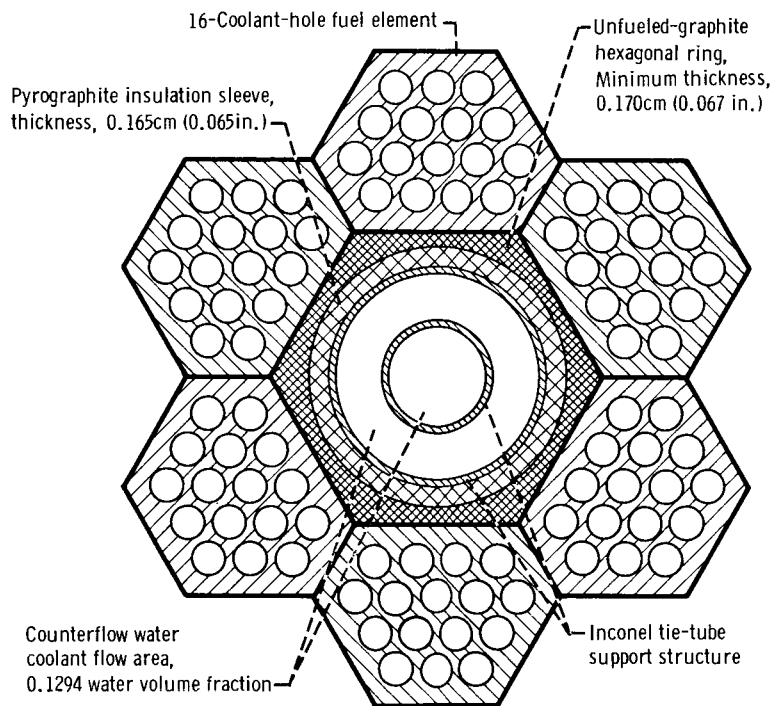


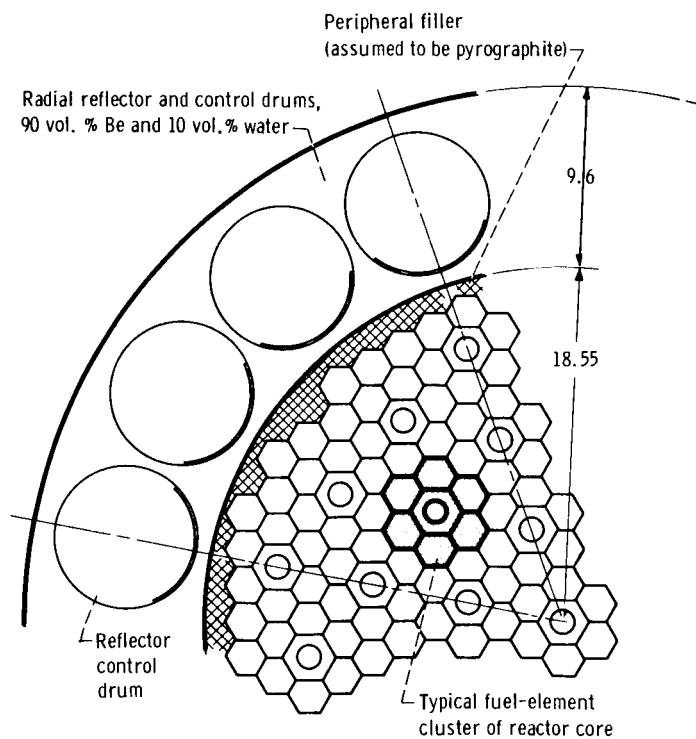
Figure 7. - Fuel-element cluster for selected core geometry. Dimensions of 16-coolant-hole fuel element, cm (in.): dimension across flat surfaces, 1.532 (0.603); coolant hole diameter, 0.292 (0.115); internal web thickness, 0.133 (0.0524); minimum web thickness at edge, 0.076 (0.030). Central tie-tube thickness, 0.038 centimeter (0.015 in.), and mean radius, 0.527 centimeter, (0.2075 in.); tie-tube liner thickness, 0.013 centimeter (0.005 in.), and mean radius, 0.985 centimeter (0.3878 in.).

void fraction would add some reactivity but would alter the assumed optimum fuel-element geometry. Even with reduced reactivity requirements for possibly lower temperature defect and 132-centimeter (52-in.) long elements with no axial power tailoring, the reactivity would not be adequate.

Detailed Calculation of Selected Core Geometry

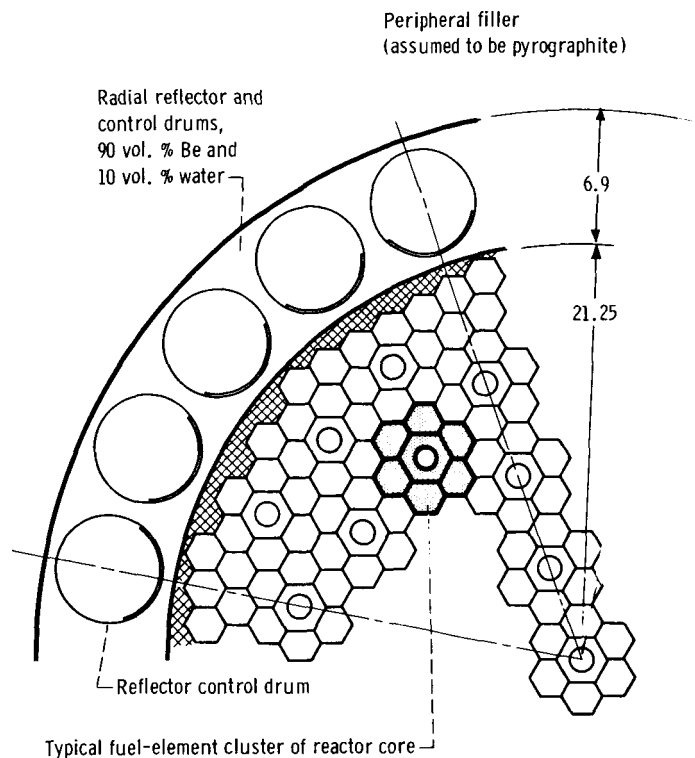
After the 0.1294-water-volume-fraction core geometry for the small water-graphite nuclear rocket was selected on the basis of a preliminary analysis, the reactors based on this geometry were calculated in greater detail by using more accurate cross sections and methods to obtain better reactor physics data. The size was extended from the 200-megawatt reactor power range to 400 megawatts to provide for an eventual performance analysis of small nuclear rocket stages over a range of powers. Size was increased by increasing the number of basic fuel-element clusters or fractions thereof and consequently increasing the core diameter.

The method for these detailed calculations is outlined in appendix A. The calculation of the homogeneous reactor-core cross sections includes the neutronic cell calculation to incorporate the relative neutron flux levels of the separate water and fueled-graphite regions. Figure 7 shows in detail both the fuel element and the various re-



(a) Reactor power, 181 megawatts.

Figure 8. - Circumferential reactor core geometry.
(Dimensions are in centimeters.)



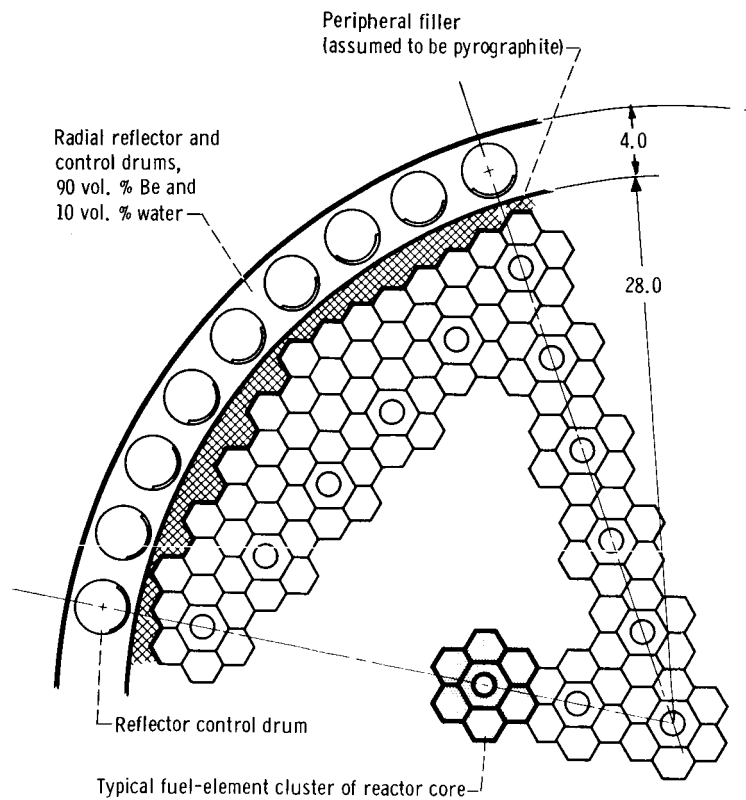
(b) Reactor power, 254 megawatts.

Figure 8. - Continued.

gions of the tie-tube-supported cluster of six fuel elements, as modified from the basic Phoebus-NERVA geometry for the selected core design.

The detailed circumferential geometry for three reactor sizes using the selected core design is shown in figure 8. These sketches were made to assess more accurately reactor power as a function of core diameter when the irregular boundary required to circularize the core lattice is incorporated. Calculations were performed for these sizes to determine the radial reflector thickness required in each case to satisfy the excess reactivity requirement. The reactivity variation with radial reflector thickness as a function of core size and reactor power is shown in figure 9 for three sizes (181, 254, and 432 MW); table IV summarizes various reactor characteristics as a function of size. The reactor power-weight ratio for these three reactors (fig. 10) shows rapid improvement with increasing core size. The asymptotic value of the power-weight ratio for an infinite core diameter, also shown in figure 10, is the ultimate attainable for this 0.1294-water-volume-fraction design.

The 432-megawatt core size requires only about 2.7 centimeters of radial reflector to meet the reactivity requirement. This thickness is somewhat below that desired for gross radial power flattening in the core-reflector interface region (about 4 cm, see



(c) Reactor power, 432 megawatts.

Figure 8. - Concluded.

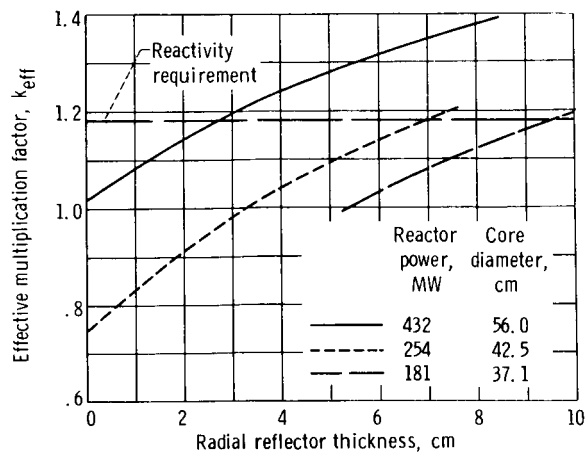


Figure 9. - Reactivity variation with core size. Uranium 233 fuel loading, 0.7 gram per cubic centimeter; water volume fraction, 0.1294.

TABLE IV. - REACTOR CHARACTERISTICS AS FUNCTION OF SIZE

[Core density, 1.604 g/cu cm; core length, 99 cm (39 in.); k_{eff} , 1.18; maximum allowable fuel-material power density, 6.84 kW/cu cm (106 Btu/(sec)(in.³)); radial and axial power factors, 1.2 and 1.362; core water volume fraction, 0.1294.]

Core power, MW	Core diameter, cm (a)	Radial reflector thickness, cm	Core weight		Radial reflector weight		Axial reflector weight		Main water plenum weight		Reactor weight		Power to reactor-weight ratio	
			kg	lb	kg	lb	kg	lb	kg	lb	kg	lb	MW/kg	MW/lb
181	37.1	9.6	171	378	252	555	35.5	78.3	39.2	86.5	498	1098	0.364	0.165
254	42.5	6.9	224	495	191	422	46.7	103	29.8	65.7	492	1086	.516	.234
432	56.0	2.7	391	862	88.8	196	80.6	178	13.8	30.5	574	1266	.755	.342
676	70	2.7	611	1348	111	245	126	278	17.3	38.2	865	1909	.781	.354
1380	100	2.7	1247	2750	159	351	258	568	24.7	54.5	1689	3724	.820	.371

^aIncludes dummy elements (see fig. 8).

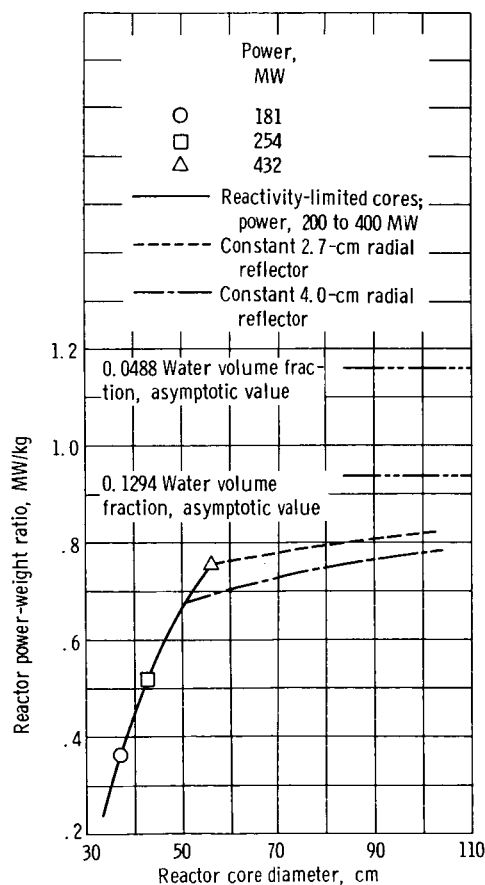


Figure 10. - Power-to-weight ratio variation with core size. Uranium 233 fuel loading, 0.7 gram per cubic centimeter.

[REDACTED]

POWER DISTRIBUTION OF SMALL CORES and fig. 12). However, if 2.7 centimeters is assumed to be the minimum possible reflector thickness, the last two rows of data in table IV represent reactor powers greater than about 400 megawatts. The trend in power-weight ratio is represented by the dashed line in figure 10.

Reactivity-limited core sizes. - The solid curve in figure 10 represents the reactivity limited cores from about 200 to 400 megawatts, where radial reflector thickness was varied to meet the reactivity requirement. The reactivity and power-weight ratio were maximized by the use of U^{233} fuel, maximum fuel loading, and optimum water volume fraction; this curve, therefore, represents the best performance for the reactivity-limited case. If lower fuel loading or U^{235} fuel were employed in the reactivity limited case, the power-weight ratio would be reduced from that shown by the solid curve in figure 10.

Core sizes greater than 400 megawatts. - The dashed curve represents core sizes greater than about 400 megawatts power, where excess reactivity is available because of the reduced radial neutron leakage. In these cases, the excess can be used to reduce fuel loading, to switch to U^{235} fuel, or to reduce water volume fraction (provided enough excess is available for the latter two incremental reactivity decreases) at no reduction in power-weight ratio. In the case of a design of lower water volume fraction, the power-weight ratio would actually increase. The asymptotic value for 0.0488 water volume fraction, which gives maximum performance, is also shown in figure 10.

Control-reactivity limitations. - The reflector thickness variation with core size must also be considered in relation to the reflector drum control required. The control requirement of 8 percent $\Delta k/k$ was estimated in the section ESTIMATION OF REACTIVITY AND CONTROL REQUIREMENTS. The radial reflector worth variation with core size from figure 9 can be compared with this requirement if an assumption is made concerning the fraction of reflector reactivity worth that is convertible to drum control reactivity. From past experience with drum control calculations in a 90-volume-percent-beryllium and 10-volume-percent-water radial reflector for the tungsten water-moderated nuclear rocket, about one-third of the radial reflector worth might be assumed recoverable for drum control. The 254- and 181-megawatt small reactors in figure 9 easily have enough reflector worth for the 8 percent control requirement. The 432-megawatt reactor, however, requires about 4 centimeters of radial reflector in order to obtain 8 percent drum worth, which would also be desirable for the gross radial power flattening effect. Four centimeters is 1.3 centimeters greater than the thickness required to meet the reactivity requirement, and reactors of about 400 megawatts power and greater become control-reactivity limited if drum control is required. The 4-centimeter reflector thickness was assumed for the 432-megawatt reactor, and the curve for that reflector thickness was included in figure 10 to illustrate the sensitivity of power-weight ratio to control requirements. For cores larger than 400 megawatts

[REDACTED]

further analysis is necessary to define (1) reflector thickness for control relative to decreasing leakage and (2) possible design changes due to the excess reactivity.

Figure 8, shows the corresponding radial reflector thickness and a possible drum control arrangement for each of the three core sizes.

POWER DISTRIBUTION OF SMALL CORES

Radial power flattening is performed to minimize the ratio of local maximum-to-average core power density and to allow more of the radial core area to operate at the maximum power-density limit. Power flattening across the core is accomplished when necessary by varying fuel loading radially from fuel element to fuel element and then matching the flow distribution to the remaining power nonuniformity by orificing. The fuel loading within the element must be constant, however, because of the fabrication technique limitations.

Steep power gradients across the fuel element itself in a power-flattened core could impose a limitation on the reactor design. The local power-density nonuniformity about coolant channels of the element can add to the thermal stress level of a uniform power density of the same average value. The gradient can result from local neutron flux perturbations due to heterogeneous core regions (e. g. , the local flux peaking of the tie-tube water regions in the center of the basic fuel-element cluster) or from the discontinuity of nuclear properties at the core - radial reflector interface. In the latter case, if the allowable power gradient is exceeded, basic core-reflector design changes (i. e. , variation of reflector thickness or ratio of core-to-reflector moderation) are required.

Even if the remaining power gradients across the core after power flattening are not steep, the maximum-to-minimum power-density fluctuation must remain within limits since the degree of orificing correction is limited. This restriction combines with that for steep gradients to specify a maximum-to-minimum power-density ratio limit.

The criteria for maximum-to-average core power-density ratio, steep power gradient, and orificing limitations, as applied to the small-core power distribution, were taken from an early Phoebus reactor study (ref. 5, pp. 92 and 94) and are supported by later practice in NERVA II (ref. 1, p. 5-2). A local maximum-to-average power-density ratio of 1.2 was considered a reasonable penalty to pay in derated average core power density for nonideal reactor radial power distribution. The limit on steep power gradients was assumed to be a ratio of maximum-to-minimum power density across a 1.915-centimeter (0.754-in.) element of 1.4, where the maximum power density was presumed to be at 1.2 times the core average power density. The same ratio, 1.4, was also applied to the overall core power distribution because of the limitation on degree of orificing.

[REDACTED]

Gross Radial Power Distribution

Unless sufficient moderation is present in the core, local radial core power density tends to peak at the core-reflector interface for strongly moderating reflectors. Small nuclear rockets with graphite cores and low core water volume fractions exhibit this peaking, although less than those with no core water content. The preliminary calculations to survey the range of water volume fraction showed these extreme power gradients at the core-reflector interface region. These power distributions are shown in figure 11

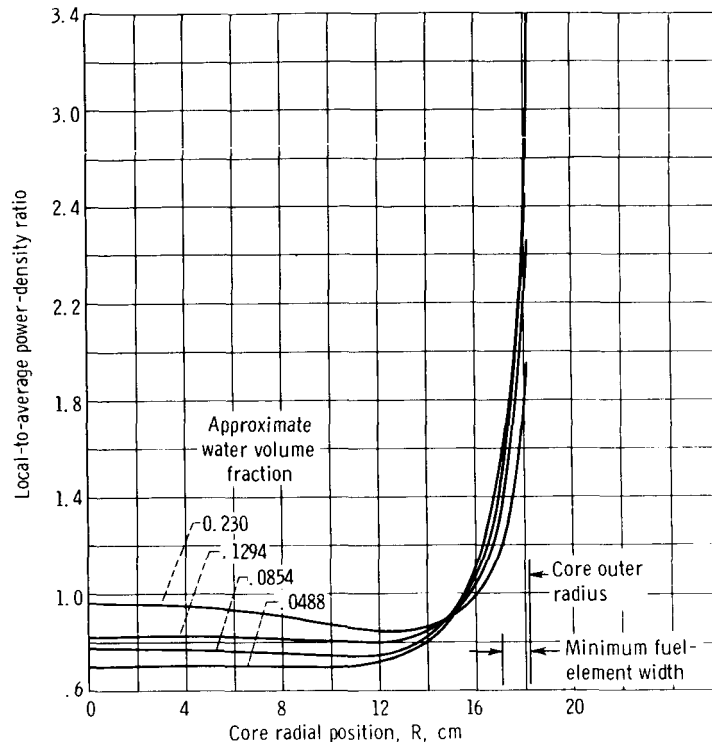


Figure 11. - Basic power-distribution trend for small water-graphite nuclear reactors. Radial reflector composition, 90 volume percent beryllium and 10 volume percent water; constant reflector thickness, 12.7 centimeters; constant core radius, 18.2 centimeters.

for the initially assumed 12.7-centimeter radial reflector thickness. The requirement for a maximum-to-minimum power-density ratio of 1.4 or less across a fuel element would probably be exceeded in every case if power flattening were attempted for a 12.7-centimeter radial reflector design.

The selected optimum core design in terms of water volume fraction (i.e., 0.1294) exhibited more moderate power gradients and, therefore, avoided this problem to a great extent. Figure 12 shows the gross radial power distribution for the three core sizes and reactor powers (181, 254, and 432 MW) for which the radial reflector thick-

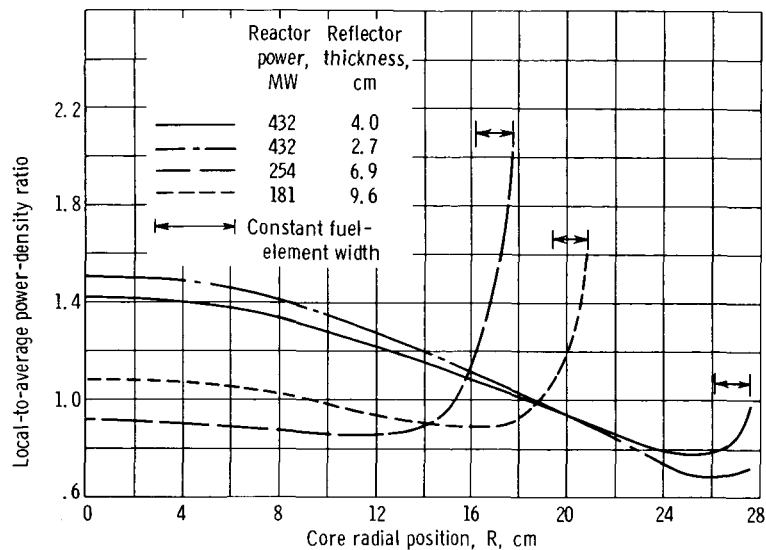


Figure 12. - Gross radial power distributions for optimum core design. Constant 0.1294-water-volume-fraction fuel-element design; reactor at ambient temperature; no average hydrogen density in reactor core; 90-volume-percent-beryllium and 10-volume-percent-water radial reflector.

ness for the reactivity requirement was determined in each case (9.6, 6.9, and 2.7 cm, respectively).

The 181-megawatt reactor with a 9.6-centimeter reflector has a power-density ratio of 1.70 over the 1.548-centimeter fuel-element width. Since the reactivity had been maximized by choice of fuel and fuel loading, the only means for attaining the allowable power gradient at this core size would be to increase the water volume fraction beyond that of the selected core design and to accept about a 27 percent power penalty (see table I, p. 14) at about the same reactor power-to-weight ratio (see table II, p. 15). If the selected core design is maintained, this core size must be rejected for exceeding the allowable power gradient, even though the reactivity requirement is satisfied.

For the 254-megawatt reactor, with a 6.9-centimeter reflector, the power-density ratio is 1.48 over the same fuel-element width. After power flattening by fuel-loading variation, the gradient in this case may decrease slightly and meet the power-gradient requirement. Therefore, this case might be considered as defining the dividing line for the core sizes limited by power gradients. More detailed analysis is required to establish the power gradient and required reflector thickness for reactivity more accurately. In appendix B, an indication of the radial variation of the spectral power and neutron flux distributions for the 254-megawatt reactor is given.

The 432-megawatt reactor with a 2.7-centimeter reflector exhibited no core-reflector interface power gradient at all. The reflector thickness was too small to reflect and thermalize a significant number of neutrons and, therefore, did not produce a neutron flux peak. The radial core power distribution approached the Bessel function shape of an unreflected, bare core. The moderate power gradient over the remainder of

[REDACTED]

the core radius was low enough for power flattening by normal fuel-loading variation from fuel element to fuel element. Therefore, the concern was to minimize the reactivity used for power flattening, by minimizing the maximum-to-minimum power-density ratio of the unflattened distribution. Increasing the radial reflector thickness to 4.0 centimeters, as shown in figure 12, did not produce an excessive power gradient but decreased the unflattened radial power-density ratio from 2.19 to 1.81. For the 432-megawatt reactor size, the 4.0-centimeter reactor was required for the control requirement discussed in the preceding section; therefore, this weight penalty of added reflector thickness can serve the two purposes simultaneously.

Cell Power Distribution

The nonuniform power distribution induced by the heterogeneous tie-tube water regions of the fuel-element cluster was investigated by performing a neutronic cell calculation which represented the cluster in an infinite array (see appendix A). The annular geometry used in the cell calculation, which approximates the actual two-dimensional geometry, maintains as separate regions the water, the Inconel tie tube, the pyrographite, the unfueled graphite, and the fuel elements (see fig. 7, p. 17). The calculated annular approximation to the power distribution radially across the fuel element is shown in figure 13. Average hydrogen coolant density was not included in the fuel-element region

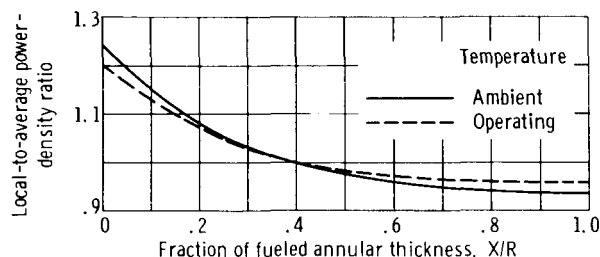


Figure 13. - Annular approximation of local power gradient in fuel-element cluster.

but is considered to have a small effect on the power shape shown in the figure. Since the cell calculation boundary condition for the fuel-element cluster is a zero neutron flux gradient, the calculated power distribution in figure 13 omits radial leakage effects on the power-distribution gradient caused by the finite reactor core size and the radial reflector. This cell power distribution must be superimposed on the flattened gross radial power distribution of the core at each cluster location to obtain the total power gradient and local maximum power density. The maximum-to-average cell power-density ratio of about 1.2 seems about low enough to combine with the flattened gross radial power distribution to meet the criteria of an overall maximum-to-average ratio of 1.2. Some

[REDACTED]

use of a neutron poison in the unfueled graphite region of the fuel-element cluster may be necessary at the critical axial and radial position in the core to reduce the water-induced peaking on the inside radius of the elements. However, neutron poisoning axially for a tailored axial power distribution could possibly serve this secondary purpose.

The cell power gradient is easily within the maximum-to-minimum limit of 1.4. This gradient may in some cases actually dampen the effect of a core-reflector interface power gradient at the periphery of the core, when superimposed on it to obtain the total power gradient. Designs of higher water volume fraction, however, may experience power gradient and maximum power-density difficulties as a result of the cell power distribution unless the accompanying distance reduction between water regions compensates sufficiently for the potential power-gradient increase of larger local water regions (e.g., fig. 3, p. 6). This potential power-gradient increase represents another possible limitation besides power-weight ratio on the selection of a core design of higher water volume fraction.

Axial Power Distribution

The 99-centimeter (39-in.) fueled core length for minimum heat-transfer length in the power-tailored condition was estimated from the axial heat-transfer design and the analysis for the tungsten, water-moderated nuclear rocket (e.g., ref. 3, pp. 189 and 268). The same length was used for the water-graphite reactors since the inlet and outlet gas temperatures, equivalent coolant-channel hydraulic diameter d_e , coolant-channel length-diameter ratio L/d_e , and flow rate per unit flow area $G = m/A$ are about the same, and axial power distribution can be tailored to the same shape.

From the heat-transfer analysis of the tungsten-water-moderated-nuclear-rocket, the optimum desired axial power distribution and the axial power distribution before final tailoring by axial fuel zoning are shown in figure 14 for the 99-centimeter (39-in.) core length. The axial power distribution obtained from the axial reflector arrangement shown in figure 4 (p. 8) combined with the selected water-graphite core design is also shown in figure 14. The general agreement between the unzoned power distribution of the two reactor types before final tailoring suggests that axial neutron poison variations can attain the final power-tailored condition in the water-graphite core design. There is a similar forward shift of the peak power-density location toward the axially reflected, core inlet end in both cases and a similar maximum-to-average power-density ratio.

Actually, the 99-centimeter (39-in.) core in the tungsten reactor case provides an extra length allowance for a tailored power distribution (including fuel zoning), which is other than the optimum desired distribution shown in figure 14. The actual fuel-zoned

[REDACTED]

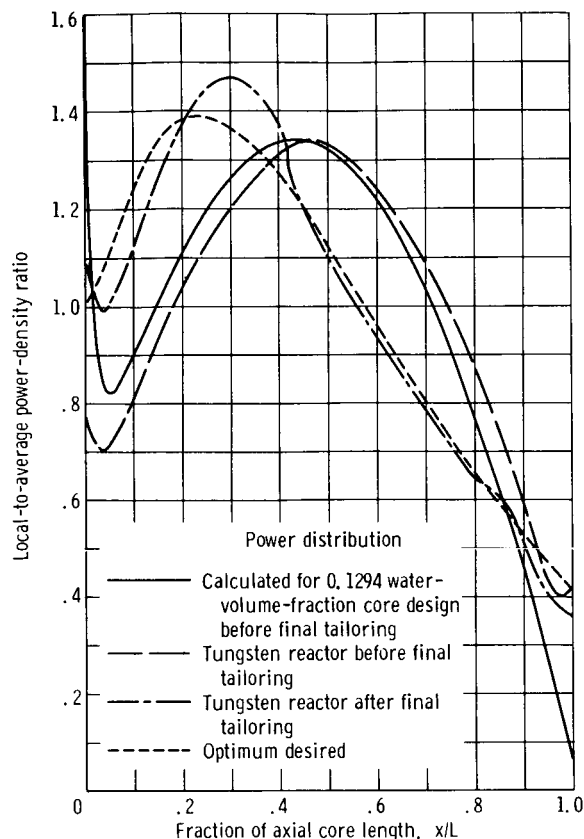


Figure 14. - Axial power-distribution comparison. Core length, 99 centimeters.

tungsten reactor axial power distribution, also given in figure 14, shows the permissible degree of flux peaking at the axial core-reflector interface.

The power distribution before final tailoring for the water-graphite reactor design shows greater flux peaking than for the tungsten reactor at the axial core-reflector interface. This peaking can be suppressed by axial thermal-neutron poisoning in the first 1 to 5 centimeters of the core at the expense of the reactivity allowed for power tailoring of the rest of the fuel element. Some relief is offered in that the 99-centimeter- (39-in. -) long fuel-element with the graphite-fuel-element heat-transfer characteristics may produce about a 15 percent reduction of the maximum surface temperature at the core inlet end with the actual tungsten-reactor fuel-zoned axial power distribution (see appendix C). This potential could be used to allow a more distorted final tailored power distribution in the water-graphite reactor.

The axial power distribution for the water-graphite reactor was obtained from a one-dimensional axial calculation which included the individual axial reflector regions shown in figure 2 (p. 5) and any reflector poisoning due to tie tubes, plenum structure, and orifice structure. Implicit in this calculation is the assumption of radial-axial neutron flux separability through the assumption of infinite radial dimensions.

TEMPERATURE DEFECT OF SELECTED CORE SIZES

The value of the temperature-defect reactivity change in going from ambient to operating temperature is strongly dependent on the particular characteristics of the reactor type considered. Rather than assume a value for the excess reactivity and control requirements from the tungsten water-moderated reactor studies, as was done for other requirements, the estimate was based on several calculations for the selected core design of 0.1294 water volume fraction. This estimate was factored into the preliminary analysis over the range of water volume fractions by an iterative process to arrive at the final selected core design. In addition, the calculations were performed for both the 181- and 432-megawatt reactor core sizes to include any dependence on core size at the selected 0.1294 water volume fraction.

The major temperature-defect components were assumed to be caused by (1) temperature change effects in the neutronic cell representing the fuel-element cluster in an infinite array and (2) core-temperature induced change of the radial leakage from the relatively small reflected core diameters. The radial leakage of these small nuclear rocket cores in the 250- to 430-megawatt power range exceeds the axial leakage by about a factor of 7. The axial core dimension was made infinite in the calculations, and the axial leakage temperature-defect contribution was assumed to be negligible. Reflector temperature change was also considered to be a negligible temperature-defect contribution.

A description of the cell and core-reflector calculations at ambient and operating temperatures for temperature-defect estimation is given in appendix A. In the cell calculations for the fuel-element cluster, any change of the relative neutron flux levels of the water and fuel-element regions with temperature was accounted for by maintaining the separate material regions of the fuel-element cluster in the neutronic cell approximation. A measure of the integrated effect of the flux level changes is shown in figure 13, where the fuel-element power distributions at ambient and operating temperatures are given.

The integrated effect on reactivity of all the cell components of the temperature defect was only about -0.0935 percent $\Delta k/k$. The overall temperature-defect results from the radial core-reflector calculations for 181- and 432-megawatt core sizes are given in table V. The radial leakage component of the temperature defect, the difference between the overall value and the cell component, was the predominant effect, as shown in the last column of table V. A 5.5-centimeter radial reflector was used for the 181-megawatt core, and a 4.0-centimeter reflector for the 432-megawatt core. The latter reflector corresponds to the reflector thickness selected for that size as a result of the preceding control and power-distribution arguments. For the 181-megawatt core, the reflector thickness required for the reactivity requirement was 9.6 centimeters

TABLE V. - TEMPERATURE DEFECT OF SELECTED CORE SIZES

[Cell temperature defect, -0.0935 percent of $\Delta k/k$.]

Reactor power, MW	Reactor core diameter, cm	Radial reflector thickness, cm	Temperature defect, percent of $\Delta k/k$	Temperature-defect radial leakage component, percent of $\Delta k/k$
181	37.1	5.5	-3.20	-3.11
181	37.1	9.6	Less negative than -3.20	Less negative than -3.11
432	56.0	4.0	-3.14	-3.05

rather than 5.5 centimeters, but, as leakage decreases for larger reflector thickness, the -3.11 percent $\Delta k/k$ leakage effect will approach zero. This 5.5-centimeter case, therefore, represents a worst case for the 181-megawatt reactor. The same trend incidentally applies to increasing core size. The leakage effect decreases toward zero, and the cell component of temperature defect is the only remaining component.

The largest overall value of -3.20 percent $\Delta k/k$ was selected as a typical value for the radial temperature-defect component estimate for the reactivity requirement. The axial leakage contribution to temperature defect may be about -0.2 percent $\Delta k/k$ judging from other calculations for a bare 132-centimeter (52-in.) core length. The effect of heating the radial reflector from ambient to operating temperature would decrease the reflector thickness in neutron mean free paths producing a slightly negative temperature-defect effect. A more negative value of -3.5 percent $\Delta k/k$ was therefore assumed for the reactivity requirement section to encompass all these aspects.

SMALL WATER-GRAPHITE REACTOR WEIGHT ESTIMATE

The variation of the major weight components of the selected core design with power was developed in table IV and figure 10. These weight components are herein developed in further detail for the 250- to 430-megawatt range and extrapolated to higher power (by reference to the NERVA I reactor design as a data point). This reactor weight variation from 200 to 1000 megawatts is intended for use in engine performance and mission analysis for unmanned missions using small nuclear upper stages.

Table VI shows a more detailed weight estimate for the 254- and 432-megawatt reactors, two of the three sizes originally calculated in table IV. The 181-megawatt reactor was rejected because of the excessive power-density gradient for the reflector

TABLE VI. - REACTOR WEIGHT COMPONENTS

Reactor component	254-MW reactor		432-MW reactor	
	Weight			
	kg	lb	kg	lb
^a Core weight (fuel elements and tie-tube support in 99-cm (39-in.) length)	214	472	379	837
Core support blocks (assumed core density, 6.35 cm (2.5 in.)	14.5	32	24.9	55
Orifice plate (approx. 0.317-cm (1/8-in.) Inconel)	3.6	8	6.3	14
Tie tubes above core (22.8 cm (9 in.) long)	5.9	13	11.3	25
Axial reflector (7.62 cm (3 in.) of 90 vol. % Be; 15.24 cm (6 in.) of water; 0.635 cm (1/4 in.) of Fe)	46.6	103	80.6	178
Axial reflector support ring	10.4	23	10.4	23
Peripheral unfueled pyrographite filler (2.2 g/cu cm)	13.6	30	15.0	33
Main water plenum	29.9	66	20.4	45
Radial reflector (90 vol. % Be and 10 vol. % water)	^b ₁₉₁	^b ₄₂₂	^c ₁₃₁	^c ₂₉₀
Miscellaneous	45.4	100	68.0	150
Total reactor weight	575	1269	747	1650
Reactor power-weight ratio, MW/kg (MW/lb)	0.441 (0.200)		0.579 (0.262)	

^aCore weight based on irregular circumferential geometry, figs. 8(b) and (c).

^bReflector thickness, 6.9 cm (2.7 in.).

^cReflector thickness, 4.0 cm (1.6 in.).

thickness which satisfied the reactivity requirements. In figure 15, these two reactor weights were plotted against the reactor power. The effect of the several limitations as applied to the optimum core design is summarized in this figure. The 254-megawatt reactor is on the borderline of the power-gradient limitation; therefore, we assumed that lower reactor powers are not practical. In figure 15, the less-detailed reactor weight estimates against power, from table VI, were plotted to illustrate the trend in reactor weight at higher powers. The selected core design and constant radial reflector thickness were maintained even though the reflector drum control was inadequate.

The NERVA I reactor weight (ref. 8, p. II-2) was uprated in power, based on the average core power density of NERVA II technology to extrapolate the two detailed weight

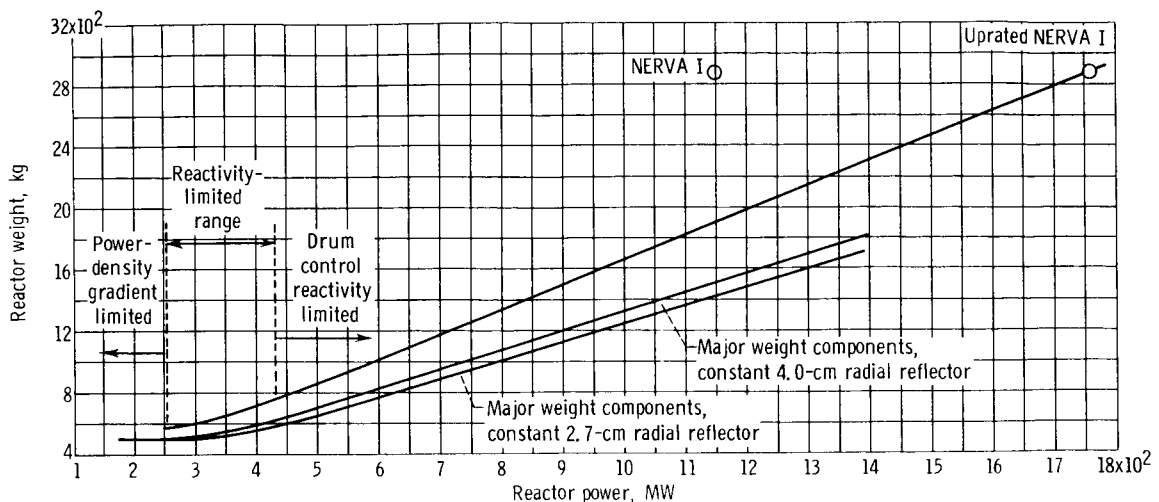


Figure 15. - Small water-graphite-reactor weight estimate. Limits apply to 0.1294-water-volume-fraction core design.

estimate points. The up-rated NERVA I data point at 1760 megawatts results from using the average core power density of the 0.0488-water-volume-fraction core design given in table I, which is a core geometry identical to the NERVA II design. Using this data point at higher power to extrapolate to 1000 megawatts was assumed to account for design changes that can arise with the available excess reactivity of the larger core sizes. This upper curve in figure 15, from 254 to 1000 megawatts, is the basis for the reactor weight estimate as a function of power for small water-graphite nuclear rockets.

AREAS FOR FURTHER STUDY

In this study of small water-graphite reactors, the major characteristics of this reactor type were analyzed, and a related estimate of reactor weight as a function of reactor power was established. Several reactor physics areas are recommended for further study to establish feasibility. Some related fabrication aspects were already discussed in pertinent sections of the report. The launch- and flight-safety aspects are considered to be similar to those of the larger NERVA II graphite reactor and are not considered in this report. The following reactor physics areas are recommended for further study:

- (1) A detailed drum control study to define more accurately the range of acceptable drum control reactivity for increasing core size
- (2) Analysis of the control-drum power distortion effects on allowable power densities as drums rotate to compensate for operational reactivity changes
- (3) Further analysis of the axial-power-distribution tailoring and associated reactivity, as well as two-dimensional effects on the axial-power-distribution predic-

[REDACTED]

tion. (Complete radial-axial flux separability was assumed. However, because of the strong radial leakage, there may be an interaction between the radial and axial-flux distribution caused by the variety of regions at the core inlet end which affect axial power distribution.)

- (4) Consideration of the reactor kinetics requirements resulting from the lower delayed-neutron fraction of U^{233} compared with U^{235} (60 percent lower).

SUMMARY OF RESULTS

The general characteristics of small water-graphite nuclear rocket reactors were analyzed within the restrictions imposed by the use of the current Phoebus II - NERVA II graphite-fuel-element technology. The basic geometry of fuel elements and fuel-element clusters was maintained as much as possible. Water was introduced by replacing the hydrogen coolant in the tie-tube area. The fuel-element dimensions and thermal-stress-limited maximum power density of NERVA II technology were employed. Use of a fuel-loading limit of 0.7 gram per cubic centimeter of U^{233} maximized the reactivity available to minimize the critical size of these reactivity-limited, high-neutron-leakage reactors.

An axial core length of 99 centimeters, corresponding to an axially tailored power distribution for minimum heat-transfer length, was assumed in all cases. A 16.5 percent $\Delta k/k$ excess reactivity requirement and an 8 percent $\Delta k/k$ control requirement were estimated for reactivity criteria in the analysis. The results of the study are the following:

1. The optimum-water-volume-fraction core design is 0.1294 for the 200-megawatt-power range, based on consideration of preliminary reactivity calculations over a water-volume-fraction range of 0.0488 to 0.230. This 0.1294 water volume fraction corresponds to a 13-coolant-channel fuel-element design, where the innermost row of 3 coolant channels was removed from the standard hexagonal Phoebus-NERVA fuel element to provide for the enlarged central tie-tube and water region.

The criterion for selection was a maximum reactor power-weight ratio. As the power level and core diameter increase, the selected water volume fraction becomes optimum by a greater margin, compared with higher water-volume-fraction designs. In the limiting case of a large reactor, the optimum shifts to even lower water volume fraction (in this study 0.0488 was the lowest fraction considered). The causes of this trend to lower water volume fraction at large reactor sizes are as follows: (1) the increasing fuel-element volume fraction of the lower water-volume-fraction designs, when the excess reactivity requirement is no longer a limitation and (2) the resulting higher average core power density and power-weight ratio.

[REDACTED]

2. Using the selected optimum core design in more detailed calculations, the reactor size and power were varied to determine the relation of excess reactivity requirements, control requirements, and power-density-gradient limitations over the range of power. Three particular core sizes and powers (181, 254, and 432 MW) established the range of size variation. The 181-megawatt reactor size satisfied excess reactivity and control requirements, but exceeded the power-gradient limitation over one fuel-element width at the core-reflector-interface power spike. The 254-megawatt reactor size is on the borderline of the power-gradient limitation, and, therefore, lower reactor powers are not considered practical for this type of core design.

From 254- to 432-megawatts these small nuclear rocket reactors are reactivity limited. When the reactivity potential of the core was maximized by use of U^{233} fuel and a maximum loading of 0.7 gram per centimeter, the minimum reflector thicknesses for the reactivity requirement were obtained. These thicknesses maximized the power-weight ratio in this range for further engine performance analysis, if the 0.1294-water-volume-fraction core design was assumed to remain optimum throughout the power range.

At about 432 megawatts and beyond, the reactor is limited not by reactivity requirement, but by the amount of reflector worth required for sufficient drum control. Also, in this power range the excess reactivity from further reduced radial neutron leakage can be used to revert to U^{235} fuel, to lower fuel loading, and/or to lower water-volume-fraction core design for higher average core power density. No attempt was made to analyze these possibilities.

3. From a detailed estimate, the 254-megawatt reactor weight would be 575-kilograms (1270 lb), and the 432-megawatt reactor weight would be 748 kilograms (1650 lb). These weights are exclusive of shielding and engine components such as control system, instrumentation, pressure vessel, nozzle, piping, and turbopumps.

4. The reactor weight estimate against reactor power for the 0.1294-water-volume-fraction core design approached an asymptotic value of about 575 kilograms (1270 lb) at the minimum allowable power of about 254 megawatts, as determined by the power-gradient limitation. Extrapolation to powers beyond 432 megawatts by reference to NERVA I reactor weight uprated to NERVA II power density gave a 1650-kilogram (3650-lb) reactor weight at 1000 megawatts.

5. The temperature-defect reactivity change from ambient to operating temperatures was about -3.5 percent $\Delta k/k$ for the 0.1294-water-volume-fraction water-graphite reactor. Essentially, all the reactivity decrease resulted from increased radial leakage.

Lewis Research Center,

National Aeronautics and Space Administration,

Cleveland, Ohio, August 25, 1967,

120-27-06-18-22.



APPENDIX A

DESCRIPTION OF REACTOR CALCULATIONS

Basic Procedure

An analytical study of the steady-state neutronics of a nuclear reactor requires the solution of coupled differential equations for the spectral and spatial variations of the neutron flux. These equations are finite-difference approximations to the general, continuous Boltzmann transport equation in neutron energy and space dimensions and are usually solved by numerical integration by a digital computer. However, one computer program generally cannot supply the entire solution, primarily because of computer storage limitations. Thus, it was necessary to make certain simplifying assumptions and approximations concerning (1) the separability of spectral and spatial variations of the neutron flux, (2) the spectral detail of the nuclear cross sections, and (3) the radial-axial spatial neutron flux distribution separability. Cross-section information was then conveyed between computer program steps isolated by the application of these assumptions.


All the reactor calculations for this study followed the same basic procedure and used the following computer program steps:

(1) Generation of thermal- and fast-neutron flux spectra and then multigroup cross sections weighted by energy spectrum from programs which solve only the energy part of the Boltzmann transport equation. The neutron flux spectra of the major reactor material regions were calculated by the following means:

- (a) Using magnetic-tape libraries of basic microscopic cross-section data (at as many intervals as possible)
- (b) Using input information on the element compositions and atom densities of representative homogeneous mixtures (generally for the reactor core and reflector)

Each spectrum was then used to flux weight the macroscopic element cross sections of the constituents of each homogeneous mixture, or the mixture itself, to form the broad multigroup cross-section format for detailed multigroup spatial flux calculations.

(2) Calculation of the multigroup, one-dimensional, radial spatial fluxes in the detailed material regions of a reactor core "cell" (defined by the basic fuel-element-cluster building block of the reactor core lattice) to obtain homogeneous, flux-weighted core cross sections. A program for the multigroup, spatially dependent form of the Boltzmann transport equation was used in this step and radial-axial spatial flux separability was assumed. The input of individual multigroup material cross-section sets was transformed by spatial flux weighting into a single set of homogeneous reactor core



(i. e., fuel-element cluster) cross sections, including the effect of the detailed cell flux perturbations.

(3) Lastly, estimation of overall reactor effective multiplication factor and radial core-reflector spatial power distributions from multigroup, one-dimensional, core-reflector spatial flux calculations. The program for the multigroup, spatially dependent form of the Boltzmann equation was used, as in step (2), but with a different flux boundary condition and with multigroup cross sections as input from steps (1) and/or (2).

In the first step, the GAM-II and GATHER-II fast- and thermal-cross-section programs (refs. 9 and 10) were the sources of basic spectrally weighted multigroup cross sections for the major material regions. The 15-energy-group structure shown in table VII defined the multigroup energy structure used. These 15-energy-group cross sections include as many as 14 down-scattering transfer cross sections for neutrons slowing down into the remaining lower energy groups. The four fast- and resonance-energy-range groups include an approximate calculation of the effective resonance ab-

TABLE VII. - 15-ENERGY-GROUP
STRUCTURE FOR MULTIGROUP
SPATIAL CALCULATIONS

Group	Lower energy boundary	
	ev	J
a ₁	^b 0.8209×10 ⁶	1.315×10 ⁻¹³
a ₂	5.5308×10 ³	8.86×10 ⁻¹⁶
a ₃	.4540×10 ³	.727×10 ⁻¹⁶
a ₄	2.3824×10 ⁰	3.82×10 ⁻¹⁹
c ₅	.5320	.852
c ₆	.3000	.481
c ₇	.2200	.353
c ₈	.1600	.256
c ₉	.1000	.1602
c ₁₀	.0800	.1282
c ₁₁	.0600	.0961
c ₁₂	.0400	.0641
c ₁₃	.0253	.0405
c ₁₄	.0150	.02405
c ₁₅	0	0

^aCross sections from GAM-II program (ref. 9).

^bUpper energy boundary of 14.918 MeV (23.9×10⁻¹³ J).

^cCross sections from GATHER-II program (ref. 10).

TABLE VIII. - ATOM AND MASS
DENSITIES OF MATERIALS

[Used for base temperature values at 300° K.]

Material	Atom or molecular density, atoms/cu cm	Mass density, g/cu cm
Water	0.0334×10 ²⁴	1.0
Inconel; vol. fraction of-	-----	8.33
Ni, 0.524	^a .0913	-----
Cr, 0.222	^a .0822	-----
Nb, 0.0495	^a .0545	-----
Mo, 0.0244	^a .0640	-----
Fe, 0.180	^a .0848	-----
Pyrographite	.1102	2.2
Graphite	.0886	1.77
NbC	.0448	7.8
U ²³³ C ₂	.0259	11.06

^aNatural atom densities of alloy elements.

~~CONFIDENTIAL~~

sorption cross sections for the coolant-channel niobium coatings in the fuel element. The Nordheim resonance absorption calculation in GAM-II was applied to the niobium by assuming a homogeneous distribution of these atoms throughout the homogenized reactor-core (i. e , fuel-element cluster) volume. The 11 thermal-energy-range-group cross sections include group-to-group scattering based on the Nelkin scattering kernel for hydrogen in water and on the Parks scattering kernel for graphite. As many as 11 upscattering cross sections treat increased neutron energy caused by scattering in the thermal-energy range. This thermal group detail is expected to calculate accurately the thermal component of the reactor fission and the power distribution in energy. The basic atom and mass densities of the different materials used in the calculations are given in table VIII for reference.

In the second and third steps, the discrete angular segmentation transport program described in reference 11 was used. These spatial calculations were confined to an S_4 order of angular segmentation and a P_0 "rational approximation" treatment of the spherical harmonic expansion of the neutron anisotropic scattering. (The rational approximation is the diagonalization of the P_1 scattering matrix, or first anisotropic term of the neutron scattering expansion, because it includes the P_1 scattering terms in the within-group scattering cross section.) This simplified calculation was used because of the preliminary nature of the calculations. Figure 3 shows the two-dimensional neutronic cell boundaries of the lattice geometry that were approximated in the cell calculation. The two-dimensional cell boundaries were converted to a one-dimensional, concentric cylindrical geometry approximation by maintaining equivalent material areas and by therefore conserving the mass of the original two-dimensional geometry.

In the cell calculation a zero-neutron-flux-gradient boundary condition at the edge of the fuel-element-cluster model was used, which implies the fuel-element cluster is in an infinite array of such clusters with neutron flux distributions produced only by material variations within the cluster. The gross radial leakage effect on flux distribution due to the finite core size and the radial reflector was therefore not included. This effect must be introduced in the final radial core-reflector calculations with zero flux boundary conditions at the outer radial reflector surface. The axial leakage in the transverse direction of the radial core-reflector calculations was treated by using the axial geometric buckling for the 132-centimeter (52-in.) core height and energy-dependent extrapolation distance $B_z^2 = \pi^2 / (132 + 1.42 \lambda_{tr})^2$. The extrapolation distance is 0.71 times the energy-dependent, material transport mean free path λ_{tr} at each end of the core.

Preliminary Reactor Calculations

The calculations performed to evaluate the water-volume-fraction effect on reactivity were based on the volume fractions of the different core materials shown in table IX. The macroscopic cross sections used for these calculations were taken from GAM-GATHER macroscopic cross sections for an earlier study of a reactor core design with a 0.29 water volume fraction and 0.4-gram-per-cubic-centimeter U^{233} fuel loading. These cross sections were then corrected for differences in atom densities. The accuracy of these calculations is considered adequate since the detailed thermal group structure minimizes any cross-section differences caused by thermalization and spectral flux weighting differences introduced by the assumed cross sections. The introduction of the detailed cell flux perturbation effects through the intermediate step of cell flux weighting was also considered to be a second-order effect unnecessary for the purposes of these survey calculations and was therefore neglected.

TABLE IX. - REGION VOLUME FRACTIONS
OF VARIOUS CORE DESIGNS

Fuel-element-cluster region	Volume fraction, V_f			
Water	0.0488	0.9854	0.1294	0.230
Inconel	.00584	.0102	.009194	.0176
Pyrographite	.0330	.0575	.05002	.0876
Graphite (unfueled)	.0553	.0967	.08509	.1428
Fuel element: Graphite ^a (fueled)	.5175	.4531	.4364	.3152
Coolant void	.3278	.2869	.2799	.1997
NbC	.01169	.01023	.009977	.007121
Total fuel element	.857	.7502	.7263	.522

^aFueled graphite contains 0.7 g/cu cm U^{233} .

Detailed Calculations of Selected Core Geometry

The selected core geometry shown in figure 7 was calculated in greater detail by the following calculational procedures:

- (1) Determining the exact volume fractions (table IX) from the dimensions of the fuel-element cluster

- [REDACTED]
- (2) Calculating in GAM and GATHER programs the fast- and thermal-neutron spectra for the exact homogeneous composition of water, carbon, U^{233} , Inconel, and niobium

- (3) Including the intermediate cell calculation

The irregular boundary of the three core sizes depicted in figure 8 was handled conservatively in the one-dimensional radial calculations. Core diameter was determined only by the fueled area up to the irregular boundary (35.50, 41.72, and 55.22 cm diameters for the 181-, 254-, and 432-MW reactors). The unfueled dummy element area used to circularize the circumference was neglected, and 2.67 percent of the core radius was added as a void region at the core-reflector interface to allow for the radial core expansion of the later temperature-defect calculations at operating temperature.

The more detailed calculations of the 0.1294-water-volume-fraction case in figure 9 required 1.6 centimeters more radial reflector thickness for the same fueled core diameter and a k_{eff} of 1.18 than did the preliminary calculations for the same case shown in figure 6. This requirement resulted from a combination of the following:

- (1) Increased reflector area at constant thickness due to the radial core-reflector expansion gap
- (2) The inclusion of flux disadvantage factors (ratio of the average flux of a material region, such as the fuel element, to the calculated average for the whole fuel-element cluster in the reactivity calculation)
- (3) Possibly, some slight microscopic group cross-section changes due to more accurate spectral weighting in the group cross-section determination

Such a trend to greater reflector thickness in detailed calculations is not expected to alter the preliminary power-weight ratio comparison given in table II.

Temperature-Defect Calculations

The calculation of the temperature-defect reactivity change from ambient (300° K) to operating temperature involved both axially infinite cell calculations and axially infinite, one-dimensional, core - radial reflector calculations at the two temperatures. The cell calculations evaluated the temperature-change effects of the detailed regions of the fuel-element cluster in an infinite array; the radial core-reflector calculations evaluated the combined cell component and radial leakage effects induced by the core-temperature changes. Then, by subtracting the cell component from the total effect, the radial leakage component was obtained since

$$\frac{\Delta k_{eff}(\Delta T)}{\bar{k}_{eff}} = \frac{\Delta k_{\infty}^{cell}(\Delta T)}{\bar{k}_{\infty}} + \frac{\Delta P_{nl}^{radial}(\Delta T)}{\bar{P}_{nl}^{radial}}$$

[REDACTED]

where

- k_{eff} overall reactor multiplication factor (axially infinite in this case), $k \propto P_{\text{nl}}$
 k_{∞} infinite cell multiplication factor
 P_{nl} radial nonleakage probability for given core and radial reflector size

and where Δ denotes the change with the ΔT temperature change in question and the bar over quantities in the denominator denotes average value over the temperature range. The radial reflector was maintained at a constant 300° K, since its temperature change and temperature effect were assumed to be negligible.

The neutronic cell calculations at ambient and operating temperatures included the temperature effects of the thermal spectrum shift and thermal-expansion and density changes. Doppler broadening of the niobium resonance absorption cross section for the niobium carbide coolant-channel coating was approximated, but the U^{233} Doppler broadening was neglected. The U^{233} Doppler broadening was assumed to be a relatively small positive or negative reactivity effect compared with the radial leakage - temperature-defect component. The change in graphite thermal scattering with temperature was represented by use of the Parks scattering kernel for graphite at 300° K and a gas kernel at 2600° K. The increase of water temperature from 300° K to an average core water temperature of 373° K was represented by a 4.16 percent decrease of atom density and use of the Nelkin scattering kernel for hydrogen in water at 300° and 373° K. The fuel-element cluster at operating temperature was defined by assuming typical average material-region temperatures and thermal-expansion coefficients and by computing the operating-temperature atom densities and dimensions of the one-dimensional heterogeneous cell model. These values are given in table X. The fuel-density reduction was

TABLE X. - FUEL-ELEMENT-CLUSTER THERMAL-EXPANSION DATA

[Base temperature, 300° K.]

Material regions	Average material operating temperature, °K	Mean thermal-expansion coefficient, α °K ⁻¹	Thermal-expansion factor	
			Linear factor, $1 + \alpha \Delta T$	Cubical factor, $(1 + \alpha \Delta T)^3$
Graphite (fueled and unfueled)	2523	^a 9.5×10^{-6} ^b 12.0×10^{-6}	^a 1.02114 ^b 1.02670	1.07639
Pyrographite	1523	9×10^{-6}	1.01103	1.03344
Inconel 718	477	7.6×10^{-6}	1.00243	1.00731

^aParallel to extrusion axis.

^bPerpendicular to extrusion axis.

[REDACTED]

obtained by using the graphite cubical expansion factor for the homogeneously distributed fuel in the fuel elements. Differential radial expansions of material regions with different expansion coefficients and average temperatures were suppressed by maintaining the fuel-element dimensional changes and by using adjusted equivalent atom densities and dimensions of other regions as necessary to maintain material contact.

In the radial core-reflector calculations the cylindrical core diameter was defined by the fueled area of the irregular core boundaries. At ambient temperature an expansion gap of 2.67 percent of the core radius, represented as a void region, was left between the core and radial reflector. This percentage corresponds to the increase of the graphite-core radial dimension from the linear thermal-expansion factor in table X. At operating temperature with the core radially expanded, no expansion gap remains, and the core extends to the original radial reflector inner radius. The core cross sections used at the two temperatures in these calculations were obtained from the homogeneous, flux-weighted, cell cross-section output of the cell calculations at the two temperatures.

APPENDIX B

SPECTRAL-NEUTRON FLUX AND POWER-DISTRIBUTION CHARACTERISTICS

When defining the general characteristics of water-graphite reactors, the spectral characteristics of this class of reactors are of interest to orient the reader with respect to his experience in fast, intermediate, and thermal reactors. These three reactor types represent the extreme range of thermalization, but a smaller variation in degree of thermalization occurs when the water volume fraction of the water-graphite reactor is varied. The neutron fluxes per unit lethargy of the fast and thermal groups as a function of their average lethargy values are shown in figure 16 to illustrate the degree of thermalization of the neutron spectra in the water-volume-fraction range (0.0488 to 0.230) of this study. These approximate spectra were taken from the 15-energy-group radial spatial calculations (12.7-cm radial reflector, 36.4-cm core diam) at the core center-line, where the spectra are primarily caused by reactor core composition. The points representing the broad energy range of about the first five groups provide only a gross indication of the fast- and resonance-energy-range spectrum but do show rather well the transition to the thermal spectrum. The lack of any Maxwellian thermal flux peaking in figure 16 illustrates the weak thermalization of this range of water volume fraction.

The high-leakage characteristic of these small nuclear rocket cores is illustrated by the low nonleakage probability P_{nl} for fission neutrons born in the core. The P_{nl} of a 0.1294-water-volume-fraction graphite reactor of 254-megawatt power is 0.560 for a k_{eff} of 1.18 (core diam, 42.5 cm; radial reflector, 6.9 cm; k_{∞} of the infinite cell, 2.1074). This low nonleakage probability, or conversely high leakage probability, and

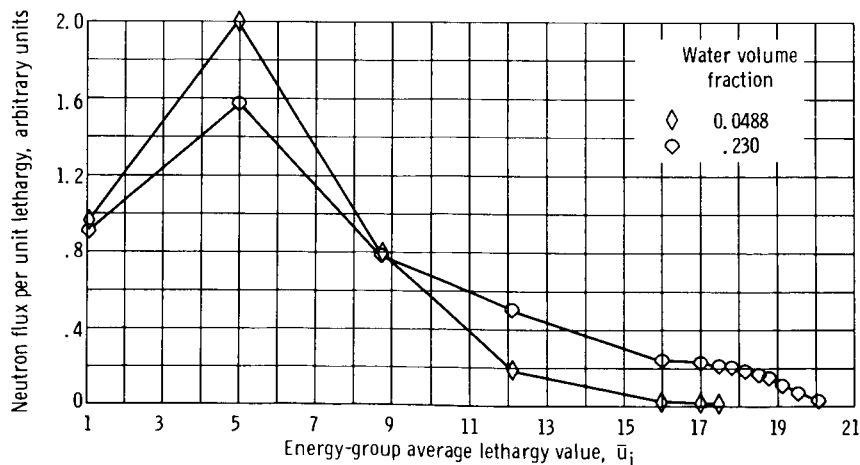


Figure 16. - Variation of neutron flux spectral distribution. Radial reflector composition, 90 volume percent beryllium and 10 volume percent water; reflector thickness, 12.7 centimeters; distributions normalized to same total flux. (Only gross indication of fast- and resonance-energy-range spectrum is given by points of first five broad groups.)

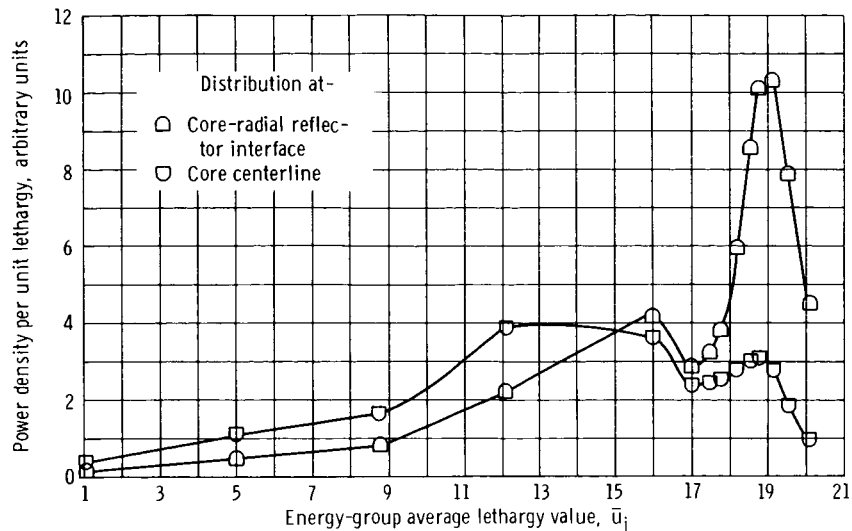


Figure 17. - Spectral power distributions of 254-megawatt water-graphite small nuclear rocket reactor. Radial reflector composition, 90 volume percent beryllium and 10 volume percent water; uranium 233 fuel isotope; reflector thickness, 7 centimeters.

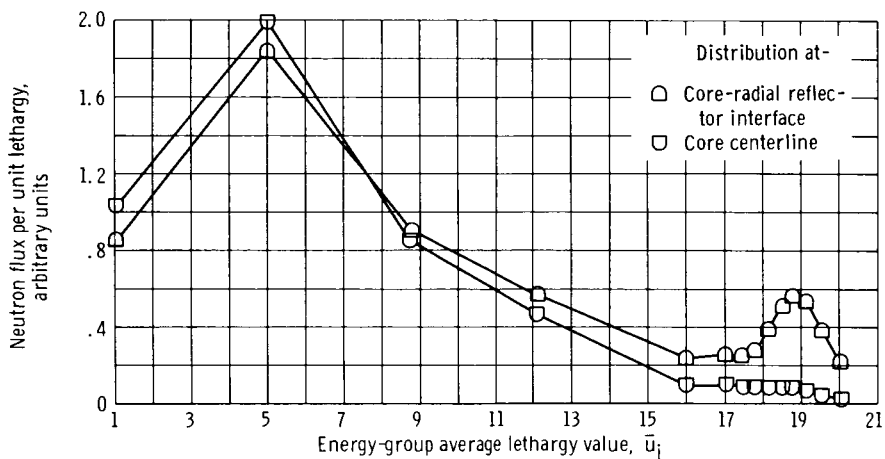


Figure 18. - Spectral neutron flux distributions of 254-megawatt water-graphite small nuclear rocket reactor. Radial reflector composition, 90 volume percent beryllium and 10 volume percent water; reflector thickness, 7 centimeters; distributions normalized to same total flux.

the radial reflection of thermalized neutrons from the radial reflector produce a strong variation of the spectral power and neutron flux distributions along the core radius. Figure 17 shows typical spectral power distributions from the 15-group core-reflector calculations for the 254-megawatt reactor with a 7.0-centimeter radial reflector. At the core centerline, the power spectrum was determined primarily by the neutron flux spectrum of the core composition and by the spectrally dependent fission cross section of U^{233} . Figure 17 shows substantial resonance- and epithermal-energy-range components of the power distribution at average lethargy values \bar{u}_i of 12 and 16 (i. e., energy groups 4 and 5 of the 15-group structure). Group 5 at $\bar{u}_i = 16$ shows the effect of the strong

[REDACTED]

1.8-electron-volt (0.288-eV) resonance of U^{233} in that group. At the radial core-reflector interface, as the curve for this case in figure 17 shows, the effect of the more thermalized spectrum on the spectral power distribution is pronounced. This curve was normalized to the same total power as for the core centerline case. With the more thermalized spectrum, the effect of the U^{233} resonance in group 5 is even more pronounced. The neutron flux spectra at these two radial positions are also shown in figure 18 for comparison. Here again, as in figure 16, only a gross indication of the fast- and resonance-energy-range spectrum is given.

APPENDIX C

AXIAL HEAT-TRANSFER COMPARISON

The heat-removal capability of the graphite fuel element was compared with that of the concentric-ring tungsten fuel element (ref. 5) to support the assumption of the 99-centimeter (39-in.) axially power-tailored core length (approaching constant wall-temperature heat transfer) in the graphite core. The heat-removal capability of the two fuel elements was compared by assuming a heat-transfer correlation applied to both fuel elements, the same axial power distribution, the same maximum allowable surface temperature T_s , and the same inlet and outlet hydrogen temperatures.

The following heat-transfer correlation,

$$\bar{h} = 0.002512 \frac{G^{0.8} T_b^{0.8}}{d_e^{0.2} T_F^{0.6}}$$

where

G mass flow rate per unit flow area, \dot{m}/A

d_e equivalent hydraulic diameter

T_b average bulk temperature, $(T_{out}^{H_2} + T_{in}^{H_2})/2$, constant for both reactors

T_F average film temperature, $(T_s + T_b)/2$

was substituted into the heat-transfer equation,

$$\frac{P_r}{\dot{m}} = \bar{h} \frac{S}{\dot{m}} (T_s - T_b)$$

where

S/\dot{m} $4 L_r/d_e G$

T_s average heat-transfer surface temperature

S heat-transfer surface area

The result is the ratio of heat-removal capability of the two fuel-element types:

$$\frac{\left(\frac{P_r}{\dot{m}}\right)_C}{\left(\frac{P_r}{\dot{m}}\right)_W} = \frac{(d_e)_W^{0.2} G_W^{0.2} \left(\frac{L_r}{d_e}\right)_C (T_s - T_b)_C}{(d_e)_C^{0.2} G_C^{0.2} \left(\frac{L_r}{d_e}\right)_W (T_s - T_b)_W}$$

if T_F is approximately constant.

TABLE XI. - TYPICAL FLOW PARAMETER VALUES

[Reactor length, 99 cm (39 in.).]

Flow parameter	Fuel element	
	Graphite	Tungsten
Coolant-hole diameter, mm (in.)	2.87 (0.113)	3.20 (0.126)
Reactor length-diameter ratio	346	310
Mass-flow rate per unit flow area, kg/(sec)(cm ²) (lb/(sec)(in. ²))	^a 0.01765 (0.251)	^b 0.0214 (0.305)


^aTypical values from NERVA II data (ref. 2, pp. 2 to 16);
reduced by 0.75, with assumption of same ratio
(Pd)_{max}/(Pd)_{av} in both 99-cm (39-in.) and 132-cm
(52-in.) reactor lengths.

^bTypical values for one concentric 10-ring fuel element.

When typical values of the flow parameters (table XI) for each fuel-element type were substituted into the ratio, a measure of the relative average and, hence, maximum surface temperatures (in the constant wall-temperature case) was obtained for reactors with the same power per unit flow rate and axial power distribution. (Power per unit flow rate was the same since $P_r/\dot{m} = \bar{C}_p (T_{out}^{H_2} - T_{in}^{H_2})$, and hydrogen inlet and outlet temperatures were assumed to be the same.) Therefore,

$$(T_s - T_b)_C = 0.844 (T_s - T_b)_W$$

and since T_b was the same for both reactors (typical $T_{in}^{H_2}$, 500° R (278° K); $T_{out}^{H_2}$, 4500° R (2500° K)), the graphite-fuel-element maximum surface temperature was about 7.5 percent lower for the average T_b and about 15 percent lower for the inlet value of T_b . (Actually, the effect of lower graphite T_s on T_F would increase the graphite heat-transfer coefficient and further reduce the graphite surface temperature relative to



that of the tungsten reactor.) This leeway could be used to compensate for further inlet-end axial-power-distribution distortion from the tungsten-reactor power-tailored distribution in figure 14.

REFERENCES

1. Anon.: Preliminary Study of the Nerva II Reactor Design. Rep. No. WANL-TME-978 978, Westinghouse Astronuclear Lab., Sept. 30, 1964.
2. Anon.: Modular Nuclear Vehicle Design. Volume I - Summary. Rep. No. LMSC-A79 A794909, Lockheed Missiles and Space Co., Mar. 3, 1966.
3. Anon.: Nuclear Rocket Technology Conference. NASA SP-123, 1966.
4. Anon.: Nuclear Rocket Program. Rep. No. ANL-7111, Argonne National Lab., 1965.
5. Houghton, W. J.; and Kirk, W. L.: Phoebus II Reactor Analysis. Rep. No. LAMS-2840, Los Alamos Scientific Lab., Apr. 16, 1963.
6. Anon.: Quarterly Status Report of LASL Rover Program for Period Ending February 28, 1967. Rep. No. LA-3679-MS, Los Alamos Scientific Lab., Mar. 31, 1967.
7. Schileo, G.: Advances in Materials - Prove Out Glovebox Fabrication of U-233. Nucleonics, vol. 24, no. 3, Mar. 1966, p. 88.
8. Anon.: Parametric Nuclear Rocket Engine Data. Vol. 5 of Mission Oriented Advanced Nuclear System Parameters Study. Rep. No. STL8423-6009-RL00, Vol. 5, TRW Space Technology Labs., 1965.
9. Joanou, G. D.; and Dudek, J. S.: GAM-II. A B_3 Code for the Calculation of Fast-Neutron Spectra and Associated Multigroup Constants. Rep. No. GA-4265, General Dynamics Corp., Sept. 16, 1963.
10. Joanou, G. D.; Smith, C. V.; and Vieweg, H. A.: GATHER-II - An IBM-7090 FORTRAN-II Program for the Computation of Thermal-Neutron Spectra and Associated Multigroup Cross Sections. Rep. No. GA-4132, General Dynamics Corp., July 8, 1963.
11. Barber, Clayton E.: A FORTRAN IV Two-Dimensional Discrete Angular Segmentation Transport Program. NASA TN D-3573, 1966.

"The aeronautical and space activities of the United States shall be conducted so as to contribute . . . to the expansion of human knowledge of phenomena in the atmosphere and space. The Administration shall provide for the widest practicable and appropriate dissemination of information concerning its activities and the results thereof."

—NATIONAL AERONAUTICS AND SPACE ACT OF 1958

NASA SCIENTIFIC AND TECHNICAL PUBLICATIONS

TECHNICAL REPORTS: Scientific and technical information considered important, complete, and a lasting contribution to existing knowledge.

TECHNICAL NOTES: Information less broad in scope but nevertheless of importance as a contribution to existing knowledge.

TECHNICAL MEMORANDUMS: Information receiving limited distribution because of preliminary data, security classification, or other reasons.

CONTRACTOR REPORTS: Scientific and technical information generated under a NASA contract or grant and considered an important contribution to existing knowledge.

TECHNICAL TRANSLATIONS: Information published in a foreign language considered to merit NASA distribution in English.

SPECIAL PUBLICATIONS: Information derived from or of value to NASA activities. Publications include conference proceedings, monographs, data compilations, handbooks, sourcebooks, and special bibliographies.

TECHNOLOGY UTILIZATION PUBLICATIONS: Information on technology used by NASA that may be of particular interest in commercial and other non-aerospace applications. Publications include Tech Briefs, Technology Utilization Reports and Notes, and Technology Surveys.

Details on the availability of these publications may be obtained from:

SCIENTIFIC AND TECHNICAL INFORMATION DIVISION
NATIONAL AERONAUTICS AND SPACE ADMINISTRATION

Washington, D.C. 20546